

Detecting Fourth Generation Quarks at Hadron Colliders

David Atwood and Sudhir Kumar Gupta

Dept. of Physics and Astronomy, Iowa State University, Ames, IA 50011

Amarjit Soni

Theory Group, Brookhaven National Laboratory, Upton, NY 11973

Although there is no compelling evidence, at present, against the Standard Model (SM), in the past few years, a number of 2-3 sigma tensions have appeared which could be alleviated simply by adding another generation of fermions. Furthermore, a fourth generation could help resolve the issue of baryogenesis and the understanding of the hierarchy problem.

In this paper, we consider the phenomenology of the fourth generation heavy quarks which would be pair produced at the LHC. We show that if such a quark with a mass in the phenomenologically interesting range of 400 GeV–600 GeV decays to a light quark and a W-boson, it will produce a signal in a number of channels which can be seen above the background from the three generation Standard Model processes. In particular, such quarks could be seen in channels where multiple jets are present with large missing momentum and either a single hard lepton, an opposite sign hard lepton pair or a same sign lepton pair.

In the same sign dilepton channel there is little background and so an excess of such pairs at large invariant mass will indicate the presence of heavy down type quarks. More generally, in our study, the main tool we use to determine the mass of the heavy quark in each of the channels we consider is to use the kinematics of the decay of such quarks to resolve the momenta of the unobserved neutrinos. We show how this can be carried out, even in cases where the kinematics is under-determined by use of the approximation, which holds quite well, that the two heavy quarks are nearly at rest in the center of mass frame.

Since it is very likely that at least the lightest heavy quark decays in the mode we consider, this means that it should be observed at the LHC. Indeed, it is expected that the mass splitting between the quarks is less than m_W so that if the Cabbibo-Kobayshi-Maskawa (CKM) matrix element between the fourth and lower generations are not too small, both members of the fourth generation quark doublet will decay in this way. If this is so, the combined signal of these two quarks will make the signal for the fourth generation somewhat more prominent.

PACS numbers: 11.30.Er, 12.60.Cn, 13.25.Hw, 13.40.Hq

I. INTRODUCTION

The Standard Model with three generations (SM3) has been very successful in explaining all experimental results to date, in particular CP violation in the K- and B-meson systems is well understood, to an accuracy of about 15-20%, in terms of the CKM matrix of that theory [1, 2]. Recently, however, some “possible evidence” for deviations from SM3 in B decays [3–8] is claimed. Although these effects can be explained by several physics beyond the Standard Model [9–15] scenarios, the simplest viable explanation seems to be an extension of the Standard Model to 4 generations (SM4) [16–22] where the mass of the new heavy quarks is in the range 400-600 GeV.

If further studies in the B system continue to show deviations from the SM3 predictions, it may be difficult to resolve which extension of SM3 is responsible. The most direct way to determine the nature of the new physics which may be involved is to produce it “on shell”. Indeed, hadron colliders, particularly the LHC, are ideally suited for this task. Since the LHC generates a significant rate of parton interactions up to energies of ~ 1 TeV it may be able to produce direct evidence of the new physics although this is not guaranteed in all cases. For instance, if the explanation lies in warped space ideas [9, 12, 13] then it appears that the relevant particles have to be at least approximately 3 TeV [23] rendering their detection at LHC rather difficult [24–26].

If the new physics is an additional sequential fourth generation, there would be two new heavy quarks, a heavy charge $+2/3$ quark (t') and charge $-1/3$ quark (b'). These quarks will be produced at the LHC predominantly by gluon-gluon fusions and should be produced at the LHC with appreciable rates [27]. For example at 10 TeV center of mass energy cross-section for pair producing 500 GeV quarks is large, ≈ 1 pb, rising to around 4 pb at 14 TeV and LHC experiments may well be able to study up to about 1 TeV [27, 28], which is well above the perturbative bound [29, 30]. We also note that experiments have already been searching for the heavier quarks and provided (95% CL) bounds: $m_{t'} \gtrsim 311$ GeV; $m_{b'} \gtrsim 338$ GeV [28, 31–36]. These bounds are a little higher than the one quoted in Ref. [37] of $m_{t'} \gtrsim 256$ GeV; $m_{b'} \gtrsim 128$ GeV at 95% CL.

For the analysis to follow an important characteristic of the fourth generation quark doublet is that the mass

splitting between the b' - and t' -quarks is constrained by electroweak precision tests to be small, likely less than m_W [38].

In addition to resolving the phenomenological hints of physics beyond SM3 that are alluded to in the above discussion, if a fourth generation is present, it may be helpful in explaining the long standing hierarchy problem within the SM. With very massive quarks in the new generation it has been proposed that electroweak symmetry breaking may well become a dynamical feature of the model [39–46].

Another issue which is naturally addressed by the presence of a fourth generation is the origin of baryogenesis in the early universe. The tiny amount of CP violation allowed in the context of the CKM matrix of SM3 is much too small to supply the CP violation necessary for baryogenesis in the early universe. However, if a fourth generation is present, then there are two more additional phases in the CKM matrix. The effects of these new phases is significantly enhanced [47] by the larger masses of the new generation and so the natural CP violation of SM4 is perhaps large enough [48–50] to satisfy that Sakharov [51] condition for baryogenesis. It has been pointed out [49], however, that in the Standard Model with a fourth generation there might not be a first order phase transition hence it may still be the case that additional physics is required to satisfy that condition for baryogenesis. The presence of the two additional phases in the SM4 mixing matrix also can have many interesting phenomenological implications especially in observables that in SM3 are predicted to yield null results [18–21, 52, 53].

Motivated by these considerations, in this paper we will consider the strategies for detecting fourth generation quarks at the hadron colliders. In Section II we present the expressions for the decay distributions of the decay of a fourth generation quarks considering, in particular the energy spectrum of the lepton that is produced by the decay of such a quark.

In Section III we discuss the various event samples which are most likely to be useful in obtaining signals of heavy quarks. In particular, we will consider signals consisting of multiple hard jets with missing momentum in combination with either one hard lepton, an opposite sign dilepton pair or a same sign dilepton pair. We also set out a set of basic cuts which are helpful in enhancing the signal with respect to the SM3 background. For each of the three kinds of event samples, we then discuss how the kinematics can be used to determine the mass of the heavy quark. In general a significant signal versus the background will be seen in a histogram of the reconstructed mass. In general we highlight two important challenges in reconstruction of the mass. First of all, in the presence of a large number of jets, there will be a potentially large combinatorial background; secondly in some cases there are not enough kinematic constraints to reconstruct the neutrino momenta which make up the missing momentum. In the case of the same sign dilepton pairs the SM3 background is much smaller than the signal which arises in b' -pair production thus an excess of high invariant mass same sign pairs is a clear signal for new physics in general and could be produced by b' -quarks.

In Section IV we discuss in detail the Standard Model (i.e. SM3) backgrounds which contribute to the event samples while in Section V we present our conclusions.

II. DECAY RATES OF HEAVY QUARKS

Let us now consider the main decay modes for the t' - and b' - quarks. A similar discussion is found in [54, 55] and in [56, 57] the threshold effects at the interface between two body and three body decays are discussed.

If the t' is more massive than the b' and the splitting is greater than m_W then the main decay mode of the t' will be $t' \rightarrow b'W$. If the splitting is less than m_W then it can decay through the three body modes $t' \rightarrow b'W^*$ where W^* is a virtual W which either decays leptonically or hadronically. The heavy top can also decay through the two body mode to lighter quarks, $t' \rightarrow bW^+$ etc.. As we shall show below, unless $V_{t'i} \leq 10^{-3}$ the two body mode will generally dominates over the three body mode. In this scenario the lighter b' should undergo a two body decay to u - or c -quarks with the relative branching ratios depending on the values of $V_{ib'}$.

If the t' is lighter than the b' ; the t' will decay via a 2 body mode to generation 1-3 quarks; in analogy with the b' case above, the relative branching ratios depend on the values of $V_{t'i}$. If the splitting is greater than m_W , the b' will decay via $b' \rightarrow t'W^-$. If the splitting is less than m_W the dominant decay mode might either be the three body mode $b' \rightarrow t'W^*$ or the two body mode to generation 1-3 quarks, $b' \rightarrow qW^-$ depending on the value of $V_{ib'}$. Again, the two body mode will dominate unless $V_{ib'} \leq 10^{-3}$.

Six scenarios for the complete decay chains of a fourth generation quark are thus possible depending on whether the relative mass of these quarks and the CKM matrix coupling to the lighter generations:

1. $m_{t'} > m_{b'} + m_W$ in which case $t' \rightarrow b'W^+$ and $b' \rightarrow qW^-$ where $q = u, c, t$ (with branching ratio depending on the CKM elements).
2. If $m_{b'} + m_W > m_{t'} > m_{b'}$ and $V_{t'i}$ is relatively large, the dominant decay of t' is $t' \rightarrow qW^+$ with a small branching ratio to the three body decay $t' \rightarrow b'W^*$. Again $b' \rightarrow qW^-$ where $q = u, c, t$.

3. If $m_{b'} + m_W > m_{t'} > m_{b'}$ but $V_{t'i}$ is small enough, the dominant decay of t' is $t' \rightarrow b'W^*$. Again $b' \rightarrow qW^-$ where $q = u, c, t$.
4. If $m_{b'} > m_{t'} + m_W$ in which case $b' \rightarrow t'W^-$ and $t' \rightarrow qW^+$ where $q = d, s, b$ (with branching ratio depending on the CKM elements).
5. If $m_{t'} + m_W > m_{b'} > m_{t'}$ and $V_{ib'}$ is relatively large, the dominant decay of b' is $b' \rightarrow qW^-$ with a small branching ratio to the three body decay $b' \rightarrow t'W^*$. Again $t' \rightarrow qW^+$ where $q = d, s, b$.
6. If $m_{t'} + m_W > m_{b'} > m_{t'}$ but $V_{ib'}$ is small enough, the dominant decay of b' is $b' \rightarrow t'W^*$. Again $t' \rightarrow qW^-$ where $q = d, s, b$.

In the scenarios where the dominant b' decay is $b' \rightarrow qW^-$, there is an important distinction between the case where $q = t$ and $q = u, c$. In the $q = u, c$ case the quark will just manifest as a single jet while in the $q = t$ case, the top subsequently decays to $t \rightarrow bW$ and the W may in turn decay leptonically or hadronically. The collider signature will thus depend on the nature of the W decay.

If the CKM matrix is not unitary (i.e. the fourth generation is not a genuine sequential generation of the SM) or if there is a further fifth generation (thus rendering the 4×4 CKM submatrix non-unitary) then there are some possible modifications to the above scenarios. If $V_{t'b'}$ is small, then in scenarios 1 and 4 it might not be the case that $t' \rightarrow b'W$ or $b' \rightarrow t'W$ are the dominant decay modes and these cases will resemble scenarios 2 and 5 respectively.

In the case $m_{b'} + m_W > m_{t'} > m_{b'}$ where $V_{t'i}$ is small enough to suppress the two body decay mode as in scenario 3, it could happen that $V_{qb'}$ for $q = u, c, t$ is sufficiently large that the mode $t' \rightarrow qW^+W^-$ becomes important. If the 4×4 CKM matrix is unitary then:

$$\sum_{i=1,3} |V_{t'i}|^2 = \sum_{i=1,3} |V_{ib'}|^2 \quad (1)$$

therefore a large $V_{qb'}$ will imply a large $V_{t'i}$ for some $i = d, s$ or b and so the two body mode must dominate. The analogous argument also applies for the decay $b' \rightarrow qW^+W^-$ in scenario 6.

A. Decay Rates

Let us now consider the two body decay of a heavy quark $q_1 \rightarrow q_2 W$ where q_1 is a fourth generation quark and q_2 is either the other fourth generation quark or a 1-3 generation quark.

The total decay rate at tree level is:

$$\Gamma(q_1 \rightarrow q_2 W) = |V_{12}|^2 \Gamma_2(m_1) \Delta(1, x_{21}, x_{W1}) (\Delta(1, x_{21}, x_{W1})^2 + (3 + 2x_{21} - 3x_{W1})x_{W1}) \quad (2)$$

where

$$\begin{aligned} x_{21} &= \left(\frac{m_2}{m_1}\right)^2 & x_{W1} &= \left(\frac{m_W}{m_1}\right)^2 \\ \Delta(a, b, c) &= \sqrt{a^2 + b^2 + c^2 - 2ab - 2bc - 2ca} \\ \Gamma_2(m_1) &= \frac{G_F}{8\pi\sqrt{2}} m_1^3 \end{aligned} \quad (3)$$

Note that in the limit that $m_2 \ll m_1$ which would be the case if $q_2 = u, d, c, s, b$, we can approximate Eqn. (2) by:

$$\Gamma(q_1 \rightarrow q_2 W) \approx |V_{12}|^2 \Gamma_2(m_1) (1 - x_{1W})^2 (1 + 2x_{1W}) + O(x_{21}) \quad (4)$$

Conversely if x_{21} is not small (i.e. for decays between the two heavy quarks or to tW) one can expand in this expression in x_{1W} :

$$\Gamma(q_1 \rightarrow q_2 W) \approx |V_{12}|^2 \Gamma_2(m_1) ((1 - x_{21})^3 + x_{21}x_{W1}(1 - x_{21})) + O(x_{W1}^2) \quad (5)$$

Let us now consider the three body decay $q_1 \rightarrow q_2 f f'$ where, in this paper, we will generally consider q_1 and q_2 to be the fourth generation quarks and $f f'$ are light fermion pairs which arise from the virtual W so $f f' = ud, cs, us, cd, e\nu, \mu\nu$ or $\tau\nu$.

At tree level,

$$\Gamma(q_1 \rightarrow q_2 f f') = |V_{12}|^2 |V_{ff'}|^2 N_c(ff') \Gamma_3(m_1) I(x_{21}, x_{W1}) \quad (6)$$

$N_c(ff') = 3$ for quark pairs and 1 for leptons; $V_{ff'}$ is the appropriate CKM element for quark pairs and 1 for lepton pairs and

$$\Gamma_3(m_1) = \frac{G_F^2}{192\pi^3} m_1^5. \quad (7)$$

The factor $I(x_{21}, x_{W1})$ is given by

$$\begin{aligned} I(x_{21}, x_{W1}) = & 12x_{1W} \left(\frac{1}{3}(1-x_{21})(2V^2 - 6x_{W1}U + x_{W1}W) + x_{W1}^2 U \log \frac{1}{x_{21}} \right. \\ & \left. + x_{W1}^2 \frac{2U^2 - x_{21}}{V} \left[\arctan \frac{1-U}{V} + \arctan \frac{U-x_{21}}{V} \right] \right) \end{aligned} \quad (8)$$

where

$$\begin{aligned} U &= \frac{1}{2}(1 + x_{21} - x_{W1}) \\ V &= \frac{1}{2}\Delta(1, x_{21}, x_{W1}) \\ W &= \frac{1}{2}(1 + x_{21} + x_{W1}) \end{aligned} \quad (9)$$

In the scenarios we are most interested in where the splitting between the two heavy quarks is not very large, the expression in Eqn.(8) is well approximated by:

$$I(x_{21}, x_{W1}) = (1 - x_{12})^5 \left(\frac{2}{5} + \frac{1}{5}(1 - x_{12}) + \frac{4x_{W1} + 3}{35x_{W1}}(1 - x_{12})^2 + O((1 - x_{12})^3) \right) \quad (10)$$

B. Decay Kinematics and Lepton Energy Spectrum for Two Body Decays

The two body kinematics together with the V-A structure of the W couplings determine the energy spectrum of the lepton arising from the two body $t' \rightarrow W^+ b$ and $b' \rightarrow W^- t$.

In the case of $b' \rightarrow t[W^+ \rightarrow \ell^+ \nu]$ the kinematic limits of the lepton energy in the rest frame of the b' are:

$$\begin{aligned} E_{max}^\ell &= \frac{1}{4m_{b'}} [m_{b'}^2 + m_W^2 - m_t^2 + \Delta(m_{b'}^2, m_t^2, m_W^2)] \\ E_{min}^\ell &= \frac{1}{4m_{b'}} [m_{b'}^2 + m_W^2 - m_t^2 + \Delta(m_{b'}^2, m_t^2, m_W^2)] \end{aligned} \quad (11)$$

Within this kinematic region, the distribution is given by:

$$\frac{d\Gamma}{dE_\ell} \propto E_\ell(E_0 - E_\ell) \quad (12)$$

where $E_0 = (m_{b'}^2 - m_t^2)/2/m_{b'}$.

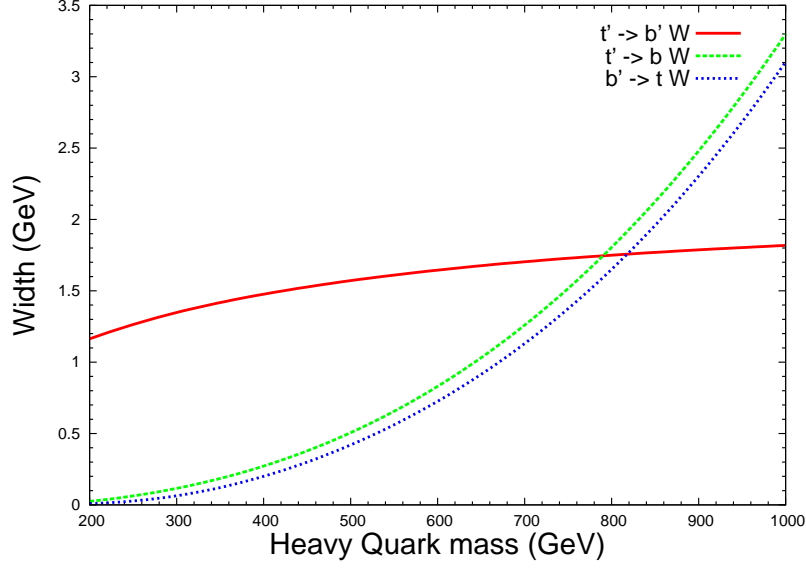


FIG. 1: The rate of heavy quark decay to specific decay modes as a function of heavy quark mass. The solid curve is $t' \rightarrow b' W$ where $m_{t'} - m_{b'} = 100$ GeV and $|V_{t'b'}| = 1$. The dashed curve is $b' \rightarrow t W$ where $|V_{tb'}| = 0.1$. The dotted curve is $t' \rightarrow b W$ where $|V_{t'b}| = 0.1$.

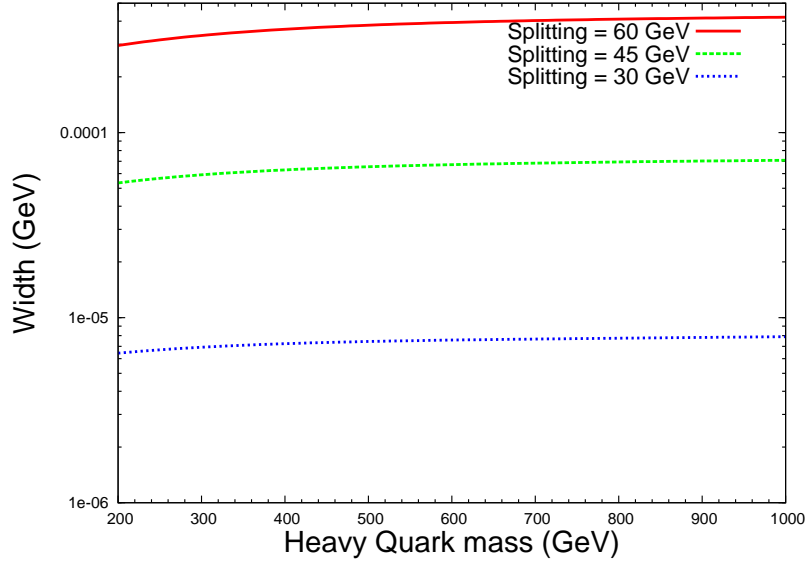


FIG. 2: The decay rate for $t' \rightarrow b' e \nu$ as a function of heavy quark mass where $|V_{t'b}| = 1$. The solid curve is for $m_{t'} - m_{b'} = 60$ GeV, the dashed curve is for $m_{t'} - m_{b'} = 45$ GeV, and the dotted curve is for $m_{t'} - m_{b'} = 30$ GeV,

From this we can calculate the average lepton energy:

$$\begin{aligned} \overline{E}_\ell &= \frac{m_{b'}}{4} \frac{1 - 3x_t + x_W + 3x_t^2 + x_W^2 - 3x_W^3 - x_t^3 - x_W x_t^2 + 5x_t x_W^2}{1 + x_W - 2x_t + x_t^2 + x_t x_W - 2x_W^2} \\ &= \frac{m_{b'}}{4} (1 - x_t) + O(x_t^2, x_W^2) \end{aligned} \quad (13)$$

where $x_W = m_W^2/m_{b'}^2$ and $x_t = m_t^2/m_{b'}^2$.

When a b' pair is produced, the matrix element and the structure functions tend to drive it to lower $\hat{s} = (p_{b'} + p_{\overline{b'}})^2$. The transverse momentum distribution of the lepton should thus be well approximated by the transverse energy distribution of the b' at rest. The average transverse momentum is thus given by:

$$\overline{P}_T^\ell = \frac{\pi}{4} \overline{E}_\ell \approx \frac{\pi}{16} m_{b'}$$
(14)

The P_T distribution in the limit where the b' is at rest is:

$$\frac{d\Gamma}{dP_T} = \begin{cases} P_T \left(E_0 \cosh^{-1} \frac{E_{max}}{P_T} - \sqrt{E_{max}^2 - P_T^2} \right) & \text{if } E_{min} < P_T < E_{max} \\ P_T \left(E_0 \cosh^{-1} \frac{E_{max}}{P_T} - E_0 \cosh^{-1} \frac{E_{min}}{P_T} - \sqrt{E_{max}^2 - P_T^2} + \sqrt{E_{min}^2 - P_T^2} \right) & \text{if } 0 < P_T < E_{min} \end{cases} \quad (15)$$

In b' -quark decay a lepton of the opposite sign may also be produced through the cascade through the top quark, $b' \rightarrow W^- [t \rightarrow b[W^+ \rightarrow \ell^+ \nu]]$. Again if the b' is at rest, we can develop an analytic expression for the energy spectrum of this lepton.

It is useful to divide the spectrum into three segments by the energies:

$$\begin{aligned} E_0 &= \frac{1}{2} m_W e^{-(\theta_t + \theta_W)} \\ E_1 &= \frac{1}{2} m_W e^{-|\theta_t - \theta_W|} \\ E_2 &= \frac{1}{2} m_W e^{+|\theta_t - \theta_W|} \\ E_3 &= \frac{1}{2} m_W e^{+(\theta_t + \theta_W)} \end{aligned} \quad (16)$$

where

$$\begin{aligned} \theta_W &= \operatorname{arccosh} \frac{x_t + x_W}{2\sqrt{x_W}} \\ \theta_t &= \operatorname{arccosh} \frac{1 + x_t - x_W}{2\sqrt{x_t}}. \end{aligned} \quad (17)$$

The energy spectrum is thus

$$\frac{d\Gamma}{dE_\ell} \propto \begin{cases} F(y, z_{max}) - F\left(y, \frac{x_W + 4y^2}{4y}\right) & \text{if } E_0 < E_\ell < E_1 \\ F(y, z_{max}) - F(y, z_{min}) & \text{if } E_1 < E_\ell < E_2 \\ F(y, z_{max}) - F\left(y, \frac{x_W + 4y^2}{4y}\right) & \text{if } E_2 < E_\ell < E_3 \end{cases} \quad (18)$$

where

$$\begin{aligned} z_{max} &= \sqrt{x_W} \cosh \theta_t + \theta_W \\ z_{min} &= \sqrt{x_W} \cosh \theta_t - \theta_W \end{aligned} \quad (19)$$

and

$$\begin{aligned} F(y, z) &= \frac{y}{4\eta} \left((2yx_t - (2y + 6yx_t + x_t)z + 8x_t(1 + y)z^2 + 4x_tz^3) \right. \\ &\quad + x_W((1 + 6y + 11x_t + 1 - yx_t) - (3 - 6yx_t + 5x_t)z - 4(1 - x_t)z^2) \\ &\quad + x_W^2((4 - 6yx_t - 10y - 7x_t) + (5 + 2yx_t + 4y + 3x_t)z + 4z^2) \\ &\quad \left. + x_W^3((2y - 6 - x_t) - (1 + 2y)z) + x_W^4 \right) \\ &\quad - \frac{y}{2} \operatorname{arccosh}(y) \left(x_t(1 + 4y) + 2x_W(1 + x_t + y - yx_t) - x_W^2(3 + x_t + 2y) \right) \end{aligned} \quad (20)$$

and $\eta = \sqrt{z^2 - x_w}$

III. EVENT SAMPLES

In order to find evidence for heavy quark pair production at hadronic colliders, we use the decay scenarios discussed above to suggest which signals should be searched for. In this discussion we would like to highlight three issues which lead to acceptance cuts that apply all the signal classes we consider. First of all, we will introduce a set of basic cuts which will preserve the signal but reduce the SM background to a manageable level (about $10\times$ signal). Next, we will consider extracting a reconstructed m_Q from the kinematics of the events that pass the basic cuts. We will see that a histogram in the reconstructed m_Q generally separates the signal from background and allows the determination of the heavy quark mass. In order to most effectively use this method, however, it is useful to reduce the combinatorial background, particularly if the signal consists of a large multiplicity of jets. As we will show, this combinatorial background can be greatly reduced due to the fact that most of the jets are in pairs resulting from W-boson decay.

Let us first consider the possible heavy quark decay modes and then turn our attention to the analysis of the cases which are likely to be of greatest experimental interest.

In general, if we assume that the heavy quark decays dominantly through a two body decay mode, the net decay of the heavy quark will be to a light quark plus 1-3 of W-bosons

If Q is the heavy quark (either a t' - or b' - quark) and q one of the five lightest quarks u, d, s, c, b , the decay chain will assume one of the following forms:

$$\begin{aligned} (1) \quad & Q \rightarrow qW \\ (2) \quad & Q \rightarrow qWW \\ (3) \quad & Q \rightarrow qWWW \end{aligned} \tag{21}$$

In particular, decay channel (1) occurs when a t' decays to a b, s or d quark and a W-boson or when a b' decays to a c or u and a W-boson. Case (1) would be the dominant b' decay mode in the mixing scenario where $V_{tb'}$ was much smaller than $V_{cb'}$ and/or $V_{ub'}$.

Conversely, the b' quark will decay dominantly through decay channel (2) if the first decay in its cascade is $b' \rightarrow tW$ where the top quark then decays to bW . The t' could also decay through a channel like this in the scenario where $m_{t'} > m_{b'} + m_W$ and the b' decayed through channel (1), thus $t' \rightarrow Wb' \rightarrow WWc$ or WWu .

Decay channel (3) would apply if the t' cascaded down to the b' which in turn decayed via channel (2). Thus $t' \rightarrow b'W \rightarrow tWW \rightarrow bWWW$.

If the mixing between the fourth and third generations is sufficiently small and the quark mass splitting is less than m_W then two other decay modes involving three body decay channels may be important:

$$\begin{aligned} (4) \quad & Q \rightarrow Q'W^* \rightarrow qWW^* \\ (5) \quad & t' \rightarrow b'W^* \rightarrow tWW^* \rightarrow bWWW^* \end{aligned} \tag{22}$$

(W^* =virtual W-boson) where in channel (4) Q is the heavier fourth generation quark and Q' is the lighter fourth generation quark.

Since the fourth generation quark Q is pair produced, depending on which of the channels above controls the decay, there are potentially up to 6 W-bosons plus 2 light quark jets in the final state. If all those W-bosons decayed hadronically, that would result in a final state with up to 14 jets. In any case the QCD background to a purely hadronic final state is likely overwhelming so we must consider cases where at least one of the W-bosons decays leptonically.

In particular, we will consider the prospect of signals where one or two of the W-bosons decay leptonically. In such a case, the signal will be a final state with one or two hard lepton(s) and significant missing momentum.

Depending on which of the channels 1-5 is dominant for each quark species, it is not unreasonable to suppose that signals of this type will received contributions from both species of quarks. This is a natural situation if the two species are roughly degenerate and so both t' and b' quarks will be produced at roughly comparable rates, especially if the masses of the b' - and t' -quarks are around 400-600 GeV and the collisions are at LHC energies, $\sqrt{s} \simeq O(7)$ TeV. Such a state of affairs can be helpful in building a signal indicating a fourth generation even before the individual contributions from t' and b' are separately identified.

The case where one or two W-bosons decay leptonically therefore leads to three signal channels for the fourth generation of quarks. We will consider the signals in each of these channels in order to determine the signal to background ratio and how the signal may be used to reconstruct the mass of the quark. These issues are related in that the difference in kinematics between SM backgrounds and the heavy quark signals means that if the mass of the quark can be reconstructed, this will provide a good mechanism for separating signals from background.

The three event samples which we consider are as follows:

1. Single lepton sample: The signature of this sample is $\ell + nj + \cancel{p}_T$ where ℓ is a lepton, either e or μ , nj means n jets and \cancel{p}_T means missing transverse momentum.
2. Like sign di-lepton sample: The signature of this sample is $\ell_1^\pm \ell_2^\pm + nj + \cancel{p}_T$
3. Opposite sign di-lepton sample: The signature of this sample is $\ell_1^\pm \ell_2^\mp + nj + \cancel{p}_T$. Note that for some of the potential SM backgrounds, it might be helpful to consider $\ell_1 \neq \ell_2$. Only heavy quarks that cascade to at least two W-bosons will contribute to this sample.

In our analysis we will consider mainly the scenario where the splitting between the two heavy quark masses is less than m_W and the CKM element between the fourth generation quarks and lighter quarks is large enough that the dominant decay mode is the two body decay to lighter quarks. Thus the decay modes for the t' and b' quarks we are mainly considering are:

$$\begin{aligned} t' &\rightarrow bW \\ b' &\rightarrow tW \rightarrow bWW \end{aligned} \quad (23)$$

which are the modes that apply if the dominant mixing of the fourth generation is with the third. The analysis we carry out however easily generalizes to the case where this assumption is weakened. Thus if the decay in fact proceeds through

$$\begin{aligned} t' &\rightarrow d \text{ or } sW \\ b' &\rightarrow u \text{ or } cW \end{aligned} \quad (24)$$

the kinematics in these cases will be identical to the t' decay to bW and so the analysis we discuss below will apply to all of these cases. In addition, if b-tagging can be carried out then we can distinguish the bW final state from u, c, s , or $d W$.

For our event analysis we first generated the signal and background events with the aid of **MadGraph** [58] and later interfaced these to **PYTHIA6** [59] for further analysis including decays of the top and W's.

For the Q -pair event generation, we wrote the **MadGraph** model files to incorporate the t' and b' and their interactions. We use **CTEQ6L** [60] to evaluate parton densities. The renormalization scale, μ_R , and the factorization scale, μ_F are fixed at

$$\mu_R = \sqrt{\hat{s}} = \mu_F \quad (25)$$

Jet formation has been done using default **PYTHIA** scheme implemented through **PYCELL**. We also incorporate effects of initial state radiation (ISR) and final state radiation (FSR) using the same simulation package.

The basic cuts that apply in these tables on leptons, $l = e, \mu$ and, jets, j (including b's) which consists of

- Lepton should have $p_{T_l} > 25$ GeV and $|\eta_l| \leq 2.7$, to ensure that they lie within the coverage of the detector.
- jets should have $p_{T_j} > 25$ GeV and $|\eta_j| \leq 2.7$
- Spatial resolution between *lepton - lepton*, *lepton - jet*, and, *jet - jet* should be $\Delta R_{ll} \geq 0.4$, $\Delta R_{lj} \geq 0.4$, $\Delta R_{jj} \geq 0.4$ respectively, (where $\Delta R_{ik} = \sqrt{\Delta \eta_{ik}^2 + \Delta \phi_{ik}^2}$, $\Delta \eta_{ik} = \eta_i - \eta_k$, $\Delta \phi_{ik} = \phi_i - \phi_k$), such that the leptons and jets are well separated in space.
- A missing transverse energy cut, $\cancel{E}_T > 30$ GeV to enhance the likelihood that leptons are due to W decay.

In addition to the cuts mentioned above, we apply the following cuts to reduce the background further:

- A minimum cut on the scalar sum of transverse momenta (H_T) of the final state lepton, jets, and the missing transverse energy of 350 GeV. H_T is defined to be:

$$H_T = p_{T_{visible}} + \cancel{E}_T = \sum_{i=l,j} p_{T_i} + \cancel{E}_T. \quad (26)$$

Quark	\sqrt{s} (TeV)	cuts	$m_Q = 300$ GeV	$m_Q = 450$ GeV	$m_Q = 600$ GeV	SM background
t'	14	<i>Basic</i>	6469, 552, 0	824, 73, 0	170, 15, 0	221833, 16479, 8.8
t'	14	<i>Basic</i> + $H_T > 350$ GeV	5571, 464, 0	809, 71, 0	169, 14, 0	46846, 3472, 6.4
t'	10	<i>Basic</i>	2404, 188, 0	272, 22, 0	49, 5, 0	63609, 4467, 4.2
t'	10	<i>Basic</i> + $H_T > 350$ GeV	2074, 158, 0	265, 21, 0	49, 5, 0	12013, 847, 3
t'	7	<i>Basic</i>	785, 61, 0	69, 6, 0	10, 1, 0	22847, 1621, 1.7
t'	7	<i>Basic</i> + $H_T > 350$ GeV	668, 50, 0	67, 6, 0	10, 1, 0	4054, 275, 1.2
b'	14	<i>Basic</i>	8948, 1210, 625	1092, 166, 86	224, 35, 18	221833, 16479, 8.8
b'	14	<i>Basic</i> + $H_T > 350$ GeV	7293, 960, 582	1057, 159, 84	221, 35, 17	46846, 3472, 6.4
b'	10	<i>Basic</i>	3312, 457, 220	370, 54, 28	65, 10, 6	63609, 4467, 4.2
b'	10	<i>Basic</i> + $H_T > 350$ GeV	2654, 358, 212	356, 52, 27	64, 10, 6	12013, 847, 3
b'	7	<i>Basic</i>	1060, 145, 74	94, 13, 7	14, 2, 1	22847, 1621, 1.7
b'	7	<i>Basic</i> + $H_T > 350$ GeV	841, 113, 70	90, 13, 7	13, 2, 1	4054, 275, 1.2

TABLE I: Number of signal and background events for a number of scenarios. In each case, the three numbers indicate the single lepton; opposite sign dileptons (OSD) and same sign dileptons (SSD) events from the t' - and b' -pair production at the LHC for $\sqrt{s} = 14, 10$ and 7 TeV and $\int \mathcal{L} dt = 1 \text{ fb}^{-1}$ without the requirement of isolation on jets. The basic cuts are: $p_{T_{l,j}} > 25$ GeV, $|\eta_{l,j}| \leq 2.7$; $\Delta R_{l,l}, \Delta R_{l,j} \geq 0.4$ and $\cancel{E}_T > 30$ GeV.

Effects of the aforementioned cuts are shown in Table I where results for both quark species are considered and results are given in the cases of $\sqrt{s} = 14, 10$ and 7 TeV. In all cases we consider the signals for heavy quark masses $m_Q = 300, 450$ and 600 GeV. In Table I we did not put any isolation cuts on the jets. In Table II we further demand that all the jets are separated with $\Delta R_{jj} > 0.4$. We see that this latter requirement does not alter the numbers very much.

Quark	\sqrt{s} (TeV)	cuts	$m_Q = 300$ GeV	$m_Q = 450$ GeV	$m_Q = 600$ GeV	SM background
t'	14	<i>Basic</i>	5906, 509, 0	747, 66, 0	152, 13, 0	204180, 14716, 7.3
t'	14	<i>Basic</i> + $H_T > 350$ GeV	5066, 416, 0	731, 64, 0	151, 13, 0	42625, 3071, 5.8
t'	10	<i>Basic</i>	2182, 172, 0	246, 20, 0	44, 4, 0	57858, 4071, 3.4
t'	10	<i>Basic</i> + $H_T > 350$ GeV	1876, 145, 0	239, 19, 0	44, 4, 0	10890, 771, 2.7
t'	7	<i>Basic</i>	704, 54, 0	62, 5, 0	9, 1, 0	20378, 1448, 1.4
t'	7	<i>Basic</i> + $H_T > 350$ GeV	597, 44, 0	60, 5, 0	9, 1, 0	3557, 233, 1.1
b'	14	<i>Basic</i>	7952, 1073, 548	982, 147, 78	201, 32, 16	204180, 14716, 7.3
b'	14	<i>Basic</i> + $H_T > 350$ GeV	6468, 843, 520	951, 142, 76	200, 32, 15	42625, 3071, 5.8
b'	10	<i>Basic</i>	2952, 403, 195	330, 49, 25	59, 9, 5	57858, 4071, 3.4
b'	10	<i>Basic</i> + $H_T > 350$ GeV	2353, 315, 189	319, 47, 24	58, 9, 5	10890, 771, 2.7
b'	7	<i>Basic</i>	935, 128, 65	83, 12, 6	12, 2, 1	20378, 1448, 1.4
b'	7	<i>Basic</i> + $H_T > 350$ GeV	738, 99, 61	80, 12, 6	12, 2, 1	3557, 233, 1.1

TABLE II: This table shows the number of events with the same cuts as in Table I with the addition of the jet isolation cut that all the jets are separated with $\Delta R_{jj} > 0.4$.

In our approach, to further enhance the signal to background ratio and characterize the fourth generation quarks, we will first consider the reconstruction of the heavy quark mass from the kinematics of the event. In this endeavor we must deal with the combinatorial background that results from the high jet multiplicity; in particular, the kinematic role of each of the jets in the event is not a priori known. This problem is most acute in the high jet multiplicities which result from b' -pair events. We then discuss the various methods which result in the reduction of this combinatorial background. We now detail our analysis in each of the signal types.

A. Analysis of Single Lepton Sample

Under our assumptions, both t' and b' decays can contribute to signals of this type.

For each event of this type, the key to determining the kinematics and therefore the heavy quark mass is the partitioning of the jets between the two Q 's in the initial state. In particular, in this case one of the heavy quarks decays only to hadrons while the others decay includes the one lepton observed. We will denote these two heavy

quarks by Q_h and Q_ℓ respectively. Thus if there are n jets, of which k should originate from the Q_ℓ then an initial $\binom{n}{k}$ combinations must be tried where only one of the possible partitions will be "correct".

In the correct partition, it is possible to determine the momentum of the unobserved neutrino. If we denote by j_h the total 4-momentum of all the jets assigned to the Q_h side of the event and j_ℓ all the jets assigned to the Q_ℓ side of the event then the following five constraints apply to the four undetermined neutrino 4-momentum:

$$\begin{aligned} (1) \quad & (\nu + \ell)^2 = m_W^2 \\ (2) \quad & (\nu + \ell + j_\ell)^2 = j_h^2 \quad (= m_Q^2) \\ (3) \quad & (\nu)^2 = 0 \\ (4) \quad & \nu_x = \not{p}_x \\ (5) \quad & \nu_y = \not{p}_y \end{aligned} \tag{27}$$

Note that if we combine equation (1) and (2) with (3) we can rephrase these two conditions as:

$$\begin{aligned} (1') \quad & \nu \cdot \ell = \frac{1}{2}m_W^2 \\ (2') \quad & 2\nu \cdot (\ell + j_\ell) + (\ell + j_\ell)^2 = j_h^2 \quad (= m_Q^2) \end{aligned} \tag{28}$$

which are linear in ν

Generally, we can use two of conditions 1-3 to solve for the t - and z -components of the neutrino momentum while 4 and 5 give the x - and y -components. The remaining condition acts as a check to ensure that we have a consistent partitioning of the jets. For example if for a given partition of the jets in each event we solve $\{1', 2', 3, 4\}$ then (because the equations are linear) we will have a unique determination of ν and therefore $|\nu|^2$ and $m_Q^2 = |j_h|^2$. Only for the correct partitions of events will the reconstruction give $|\nu|^2 \approx 0$. Thus if we plot all possible reconstructions on a scatter plot of $|\nu|^2$ versus $|j_h|^2$ and accept only those events in a strip near $|\nu|^2 \approx 0$ we should find an accumulation of events near the real value of m_Q . Those events outside of the strip are presumably background or wrongly partitioned events. If there were data from two (or more) quarks mixed together in the sample, then there would be multiple peaks corresponding to the masses of each of the quarks present. Since all of the decay channels 1-5 can contribute to this sample, this method will ultimately determine all of the fourth generation masses regardless of which mixing scenario applies.

In Figure 3 we show Leggo plots of the reconstructed m_Q versus reconstructed m_ν for a number of different scenarios. For the correct partitioning of the jets the events would indeed be at the physical values of m_Q and m_ν but not so for the incorrect partitions.

Returning to Eqn. 27 we can also use two slightly different approaches to reconstructing the quark mass which may offer some advantages. If we start with constraints $\{1, 3, 4, 5\}$ then on each event we extract the apparent masses of each side of the event: $m_{Q_1}^2 = (\ell + \nu + j_\ell)^2$ and $m_{Q_2}^2 = j_h^2$. We then check condition 2 by constructing an $m_{Q_1}^2$ versus $m_{Q_2}^2$ scatter plot. The correct partitions will be near the diagonal $m_{Q_2}^2 \approx m_{Q_1}^2$, implementing condition 2, and the quark mass or masses will be revealed as accumulations in $\overline{m}_Q = \frac{1}{2}(m_{Q_1}^2 + m_{Q_2}^2)$. In this method, for each event the neutrino momentum is determined independently of the partitioning of the jets. However, since the equations are quadratic, there is a two fold ambiguity in the solution so on the scatter plot two points must be plotted for each partitioning of each event increasing the combinatorial background.

In Figure 4 we show a histogram of m_{Q_1} versus m_{Q_2} for the t' and b' cases. Again the peaks at the correct value of m_Q correspond to correct partitioning of the jets.

In Figure 5 we illustrate another approach which is to solve the equations $\{2, 3, 4, 5\}$ and then reconstruct the W mass as $(m_W^{recon})^2 = (\nu + \ell)^2$. As with the above method the equations here are quadratic giving an additional 2 fold ambiguity. In this approach the resulting scatter plot will be in $(m_W^{recon})^2$ and j_h^2 where the correct partition will be in a strip near $m_W^{recon} \approx m_W$. The heavy quark mass or masses can be extracted from accumulations in j_h^2 . This approach has the advantage that if there were another (beyond the SM) particle playing the role of the W -boson in the Q decays such as a charged Higgs, an additional W boson or a Kaluza-Klein excitation of the W -boson, this would be evident in additional accumulations of events in the m_W^{recon} variable.

Conversely, using this method, if decay channels (4) or (5) are significant, the case where virtual W -boson decays to $\ell\nu$ will lead to additional points on the scatter plot with the correct value of j_h^2 but with $m_W^{recon} < m_Q - m_{Q'} < m_W$.

In enumerating the various jet partitions for a given event, it is useful to combine equations (1') and (2') which leads to the inequality:

$$j_h^2 \geq m_W^2 + 2j_\ell \cdot \ell + j_\ell^2 \tag{29}$$

where this inequality will eliminate at least half of the possible partitions.

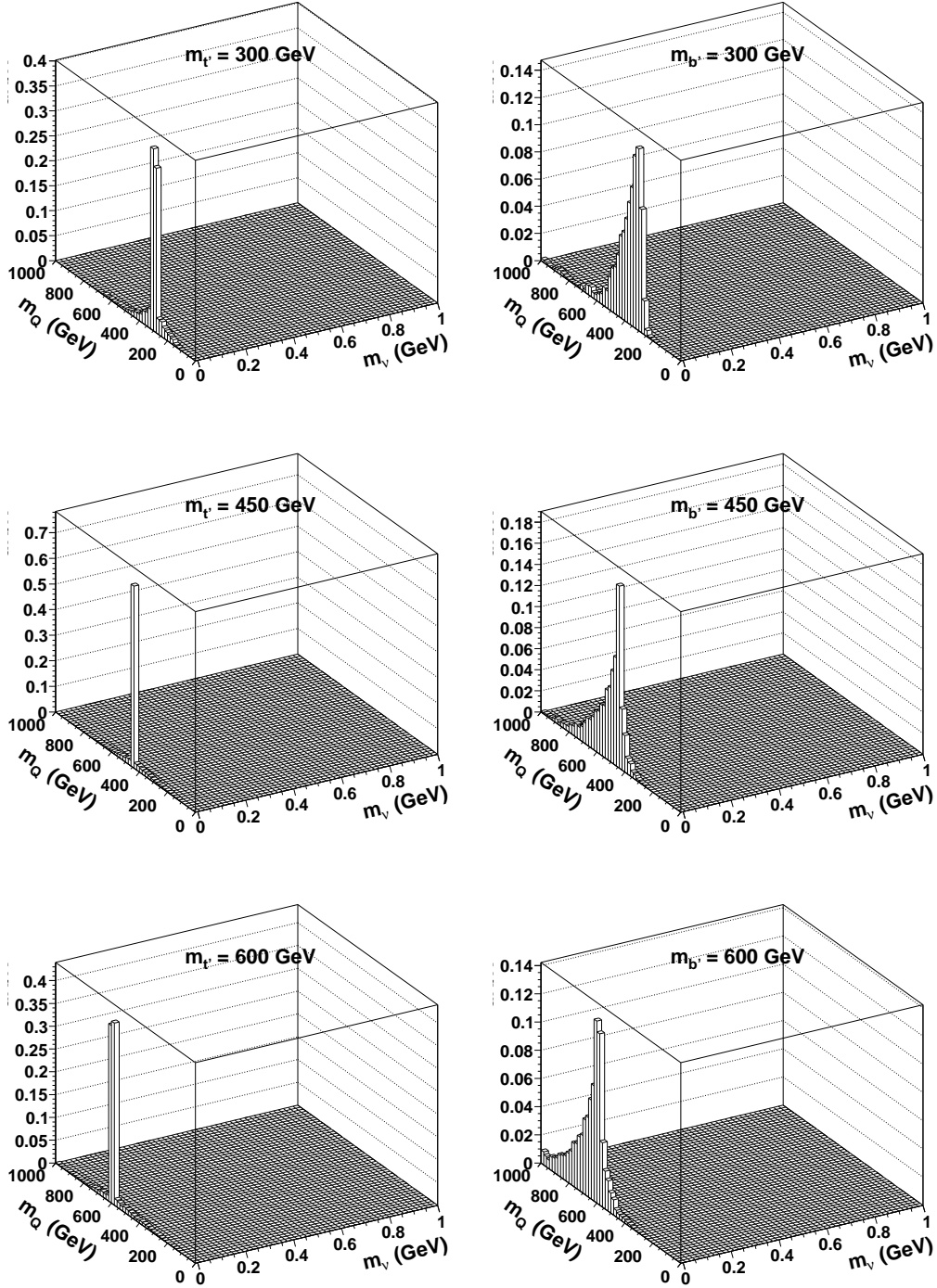


FIG. 3: 2D histogram for reconstructed m_ν and m_Q from single lepton signal after selecting events. Left plot is for t' -quarks and right is for b' -quarks.

Let us now see how to use such kinematics to enhance the signal to background. For this, we will start with the method where we solve 1,3,4,5 to determine m_{Q1} and m_{Q2} . For a given partition of the jets, we define $\Delta m_Q = |m_{Q1} - m_{Q2}|$. For a given event, we will select the reconstructed value of m_Q , m_Q^{recon} to be the value of \bar{m}_Q corresponding to the partition with the minimum value of Δm_Q .

Another cut which may be helpful in limiting the combinatorial background is to first pair up the jets in pairs with roughly the W mass. For example in the t' case there must exist one pair of jets which results from the decay of a

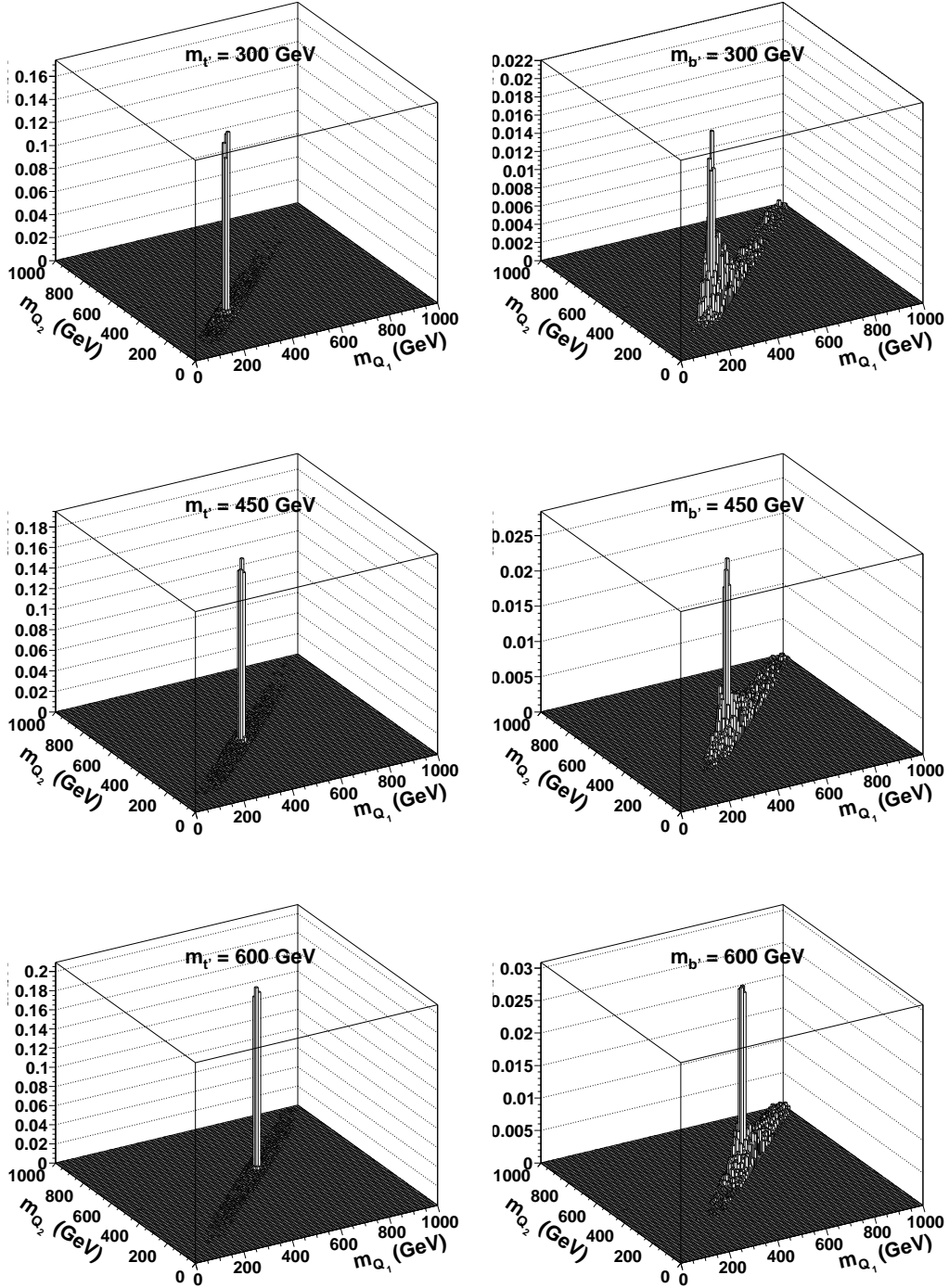


FIG. 4: 2D histogram for reconstructed $m_{Q_h}(m_{Q_2})$ and $m_{Q_\ell}(m_{Q_1})$ from single lepton signal after selecting events. Left plot is for t' -quarks and right is for b' -quarks.

W-boson and therefore should have an invariant mass of m_W . Let us denote the deviation of such a jet pair from m_W by, $\Delta m_W = m_W - m_{2jets}$, so using this cut, we would only consider partitions of jets where $|\Delta m_W|$ was smaller than some threshold. In the case of b' this cut is more constraining since it would apply to three different jet pairs in a given jet assignment.

In Figure 6 we show a histogram of the reconstructed t' mass using this method. In the cut on the upper left we just use the basic cuts. In the two plots on the right we use the cut $\Delta m_W < 15$ GeV while in the lower two plots

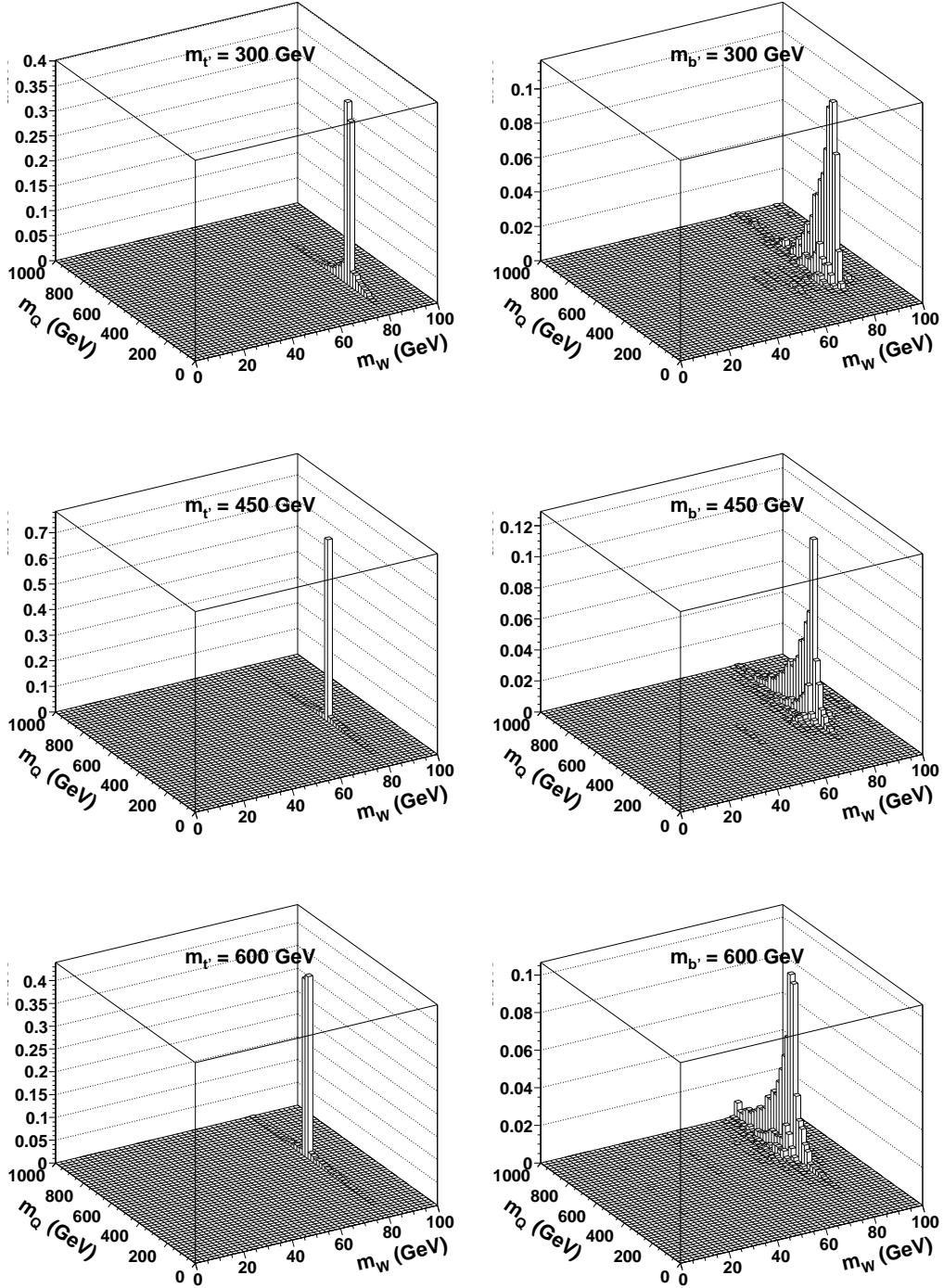


FIG. 5: 2D histogram for reconstructed m_W and m_Q from single lepton signal after selecting events. Left plot is for t' and right is for b' .

we impose the H_T cut. Thus the graph on the lower right has both cuts imposed. The plots are shown for the SM background and for $m_{t'} = 300, 450$ and 600 GeV. Clearly the signal peaks well above background and the H_T cut appears helpful in enhancing this further.

In Figure 7 we apply the same method to the case of b' and again the mass peak is well above the background and the signal is further enhanced by the H_T cut. In Figure 8 we consider the same method in the case where we consider the total signal where both species contribute. As an illustration here we are assuming that $m_{b'} = 450$ GeV

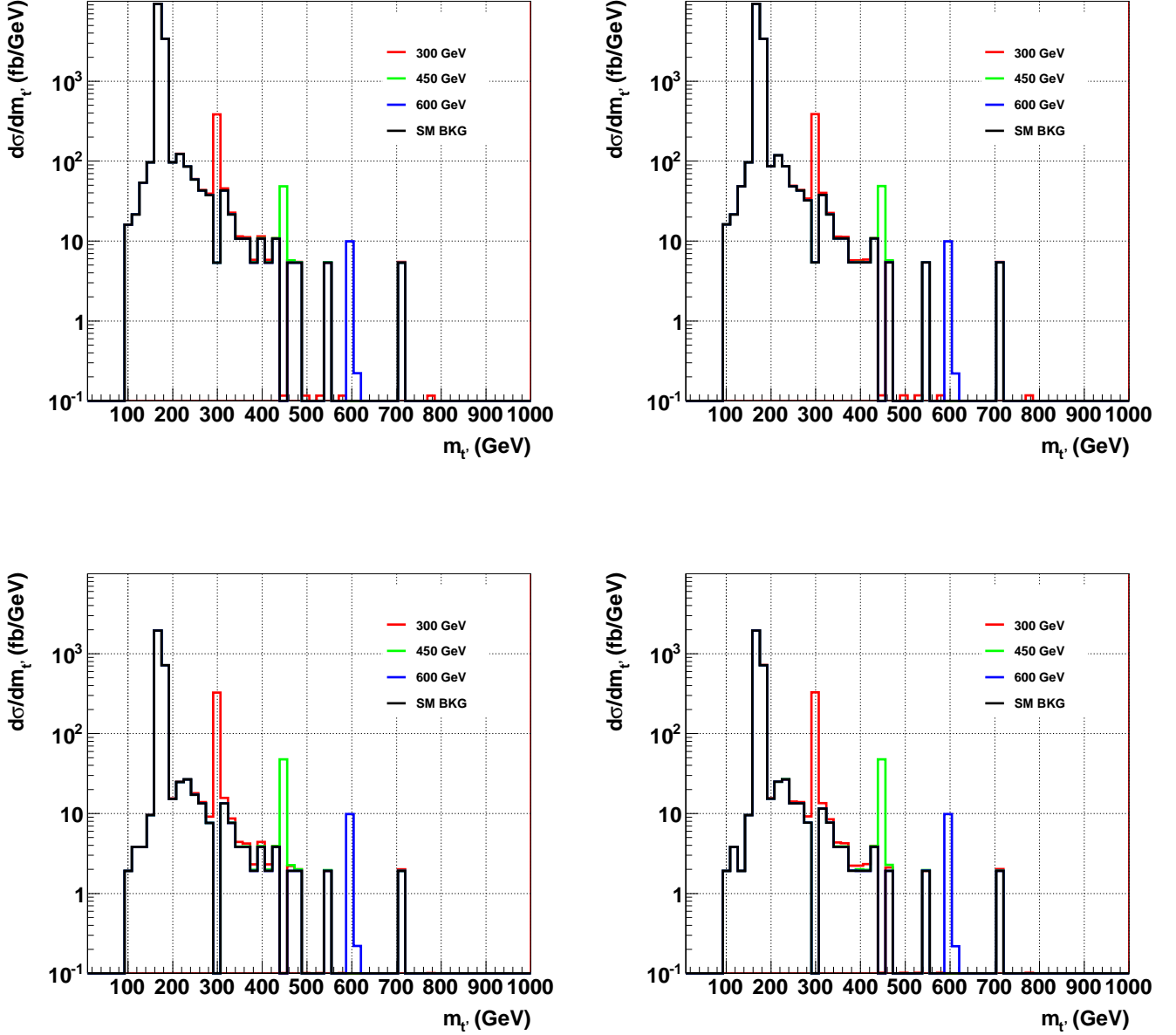


FIG. 6: Reconstructed t' masses from single lepton case. Signal plots also include the SM background. Upper two plots are with only basic cuts while the lower two plots are with basic + H_T (i.e. H_T = the scalar sum of transverse momenta of the final state lepton, jets, and the missing transverse energy) cut. In each case right plots assume W reconstruction with $|\Delta m_W| < 15$ GeV while the left plots are without W reconstruction. In all the plots we choose only that permutation in an individual event where the $|m_{Q_1} - m_{Q_2}|$ is minimum.

and $m_{t'} = 500$ GeV. The close mass of the two quarks gives a signal which is larger than we would get if just one quark contributed (see also [61]).

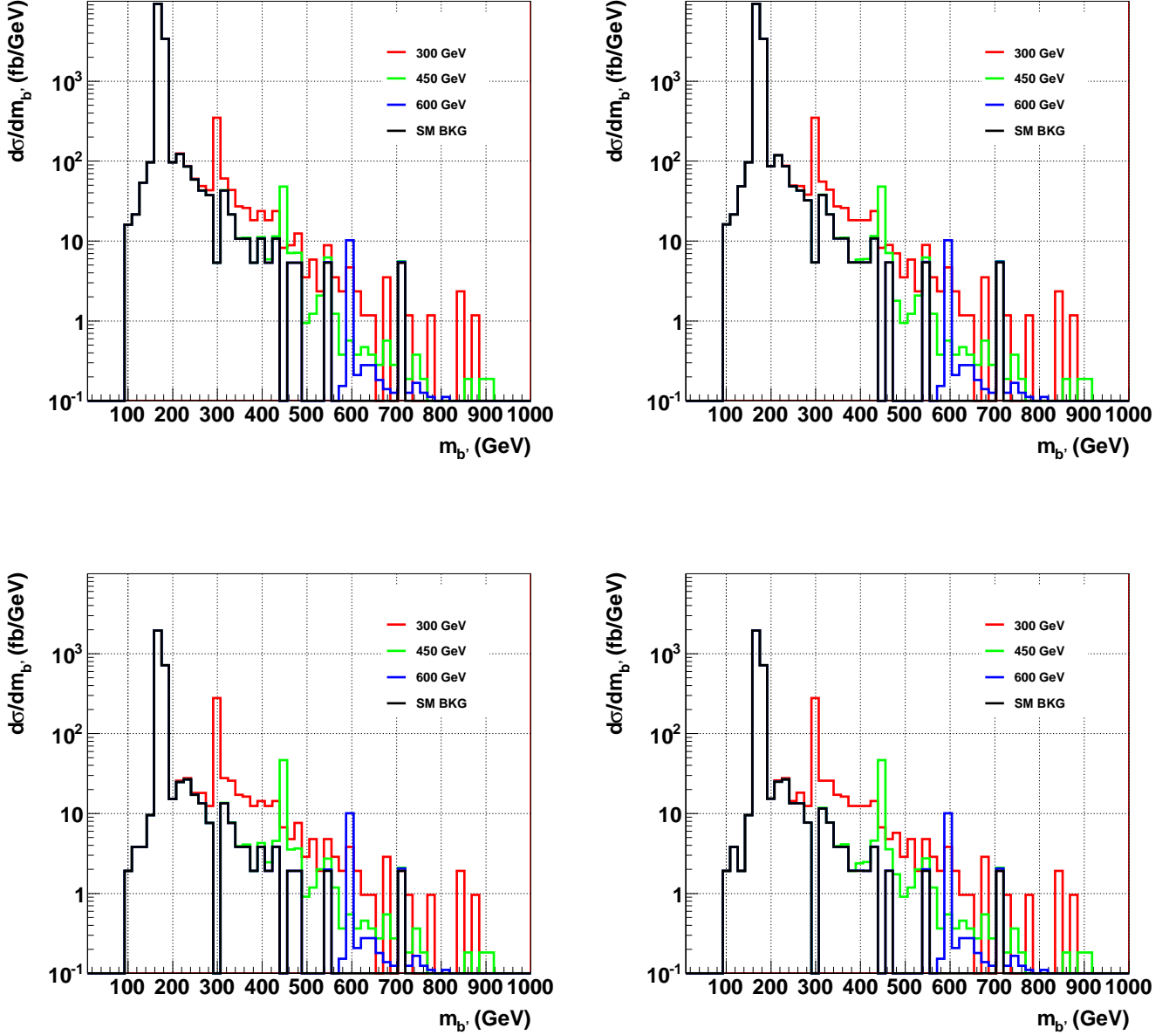


FIG. 7: Reconstructed b' masses from single lepton case. Signal plots also include the SM background. Upper two plots are with only basic cuts while the lower two plots are with basic + H_T (i.e. H_T = the scalar sum of transverse momenta of the final state lepton, jets, and the missing transverse energy) cut. In each case right plots assume W reconstruction with $|\Delta m_W| < 15$ GeV while the left plots are without W reconstruction. In all the plots we choose only that permutation in an individual event where the $|m_{Q_1} - m_{Q_2}|$ is minimum.

B. Dilepton signals

If two of the W -bosons in the decay chains we are considering decay leptonically there will consequentially be two leptons in the final state. If those two W -bosons are of opposite sign then the lepton pair will therefore be of opposite sign while if the two W -bosons are of the same sign then the pair will likewise be of the same sign. Due to the simplifying assumptions we are making, this latter case only occurs in the decay chain of b' -quark pairs. Below we will consider the problem of extracting the heavy quark mass from the kinematics in a dilepton signal while here we

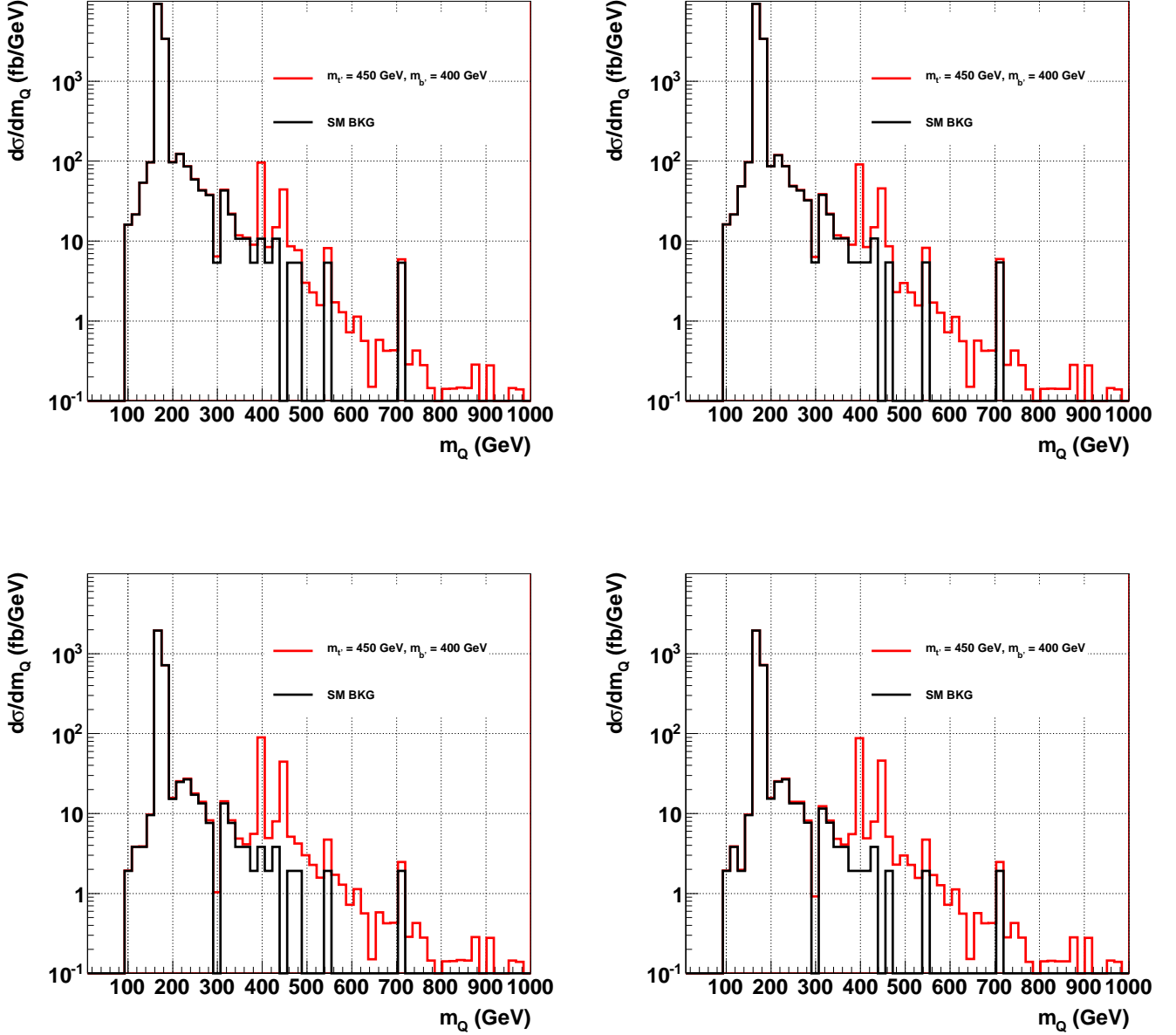


FIG. 8: Reconstructed quark mass from the combined signals of a t' - and b' -quark in the single lepton case. Signal plots also include the SM background. Upper two plots are with only basic cuts while the lower two plots are with basic + H_T (i.e. H_T = the scalar sum of transverse momenta of the final state lepton, jets, and the missing transverse energy) cut. In each case right plots assume W reconstruction with $|\Delta m_W| < 15$ GeV while the left plots are without W reconstruction. $m_{t'} = 450$ GeV and $m_{b'} = 400$ GeV are assumed here. In all the plots we choose only that permutation in an individual event where the $|m_{Q_1} - m_{Q_2}|$ is minimum.

will consider the characteristics of the signal itself.

Hard leptons are often part of the signal of new physics. In this case, the dileptons would be produced in association with jets and missing momentum. To study this signal (for opposite sign and like sign), we selected Montecarlo events passing the basic cuts described above and also imposed the cut that $H_T > 350$ GeV.

In Figure 9 we plot the invariant mass spectrum for opposite sign dilepton pairs in the case of b' - and t' -quarks of mass 450 and 600 GeV as well as the case with both species present where $m_{b'} = 400$ GeV and $m_{t'} = 450$ GeV.

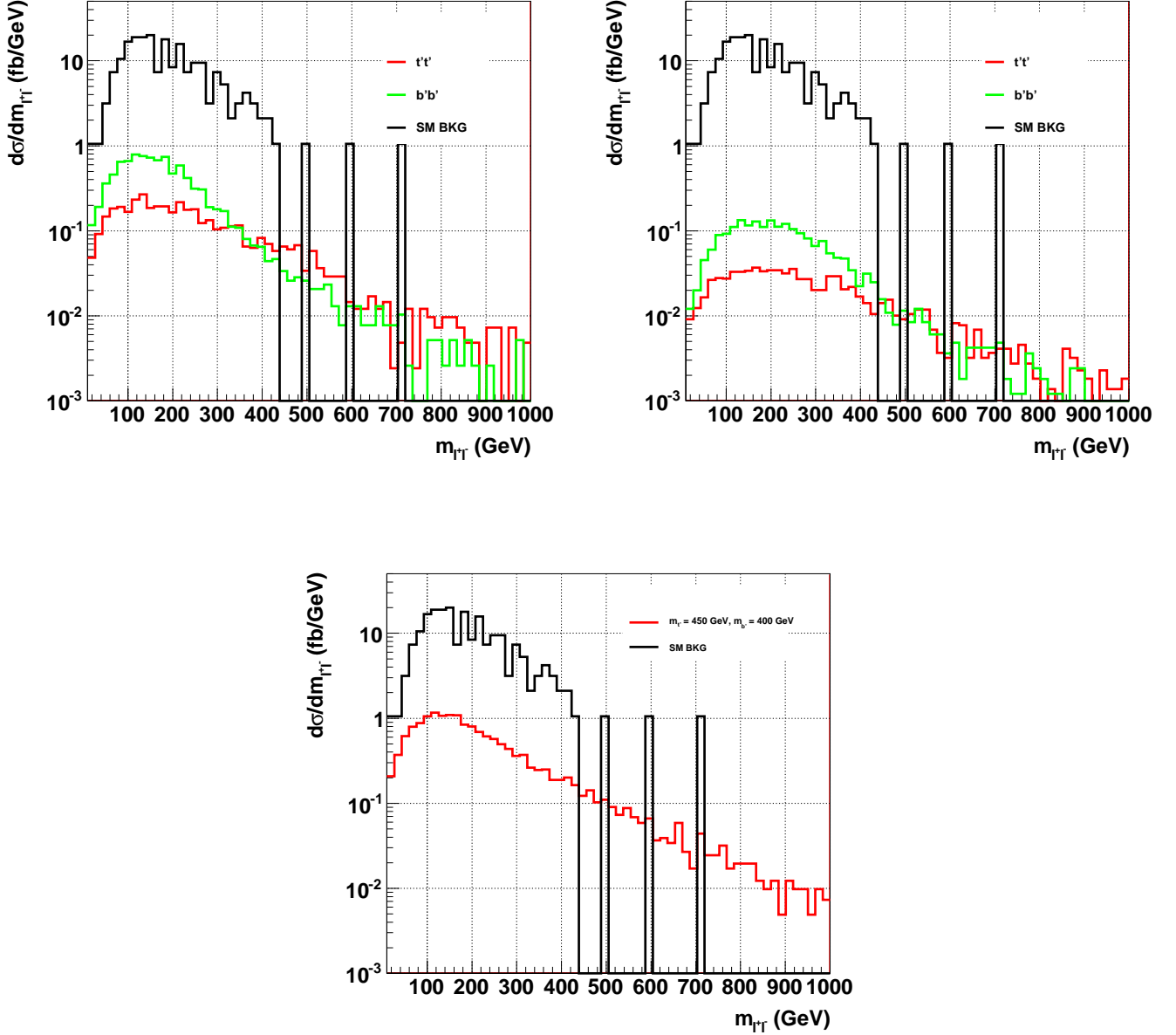


FIG. 9: m_{l+l-} distributions for OSD (opposite sign dileptons) cases with $m_Q = 450$ (top left), $m_Q = 600$ (top right) and combined case with $m_{l'} = 450$ and $m_{b'} = 400$ GeV (bottom).

Note that the t' decay gives rise to harder leptons because both of the leptonic W-bosons arise from the primary decay while in the b' case the spectrum is softer because some of the leptonic W-bosons arise from secondary top decay. Likewise the overall rate for the b' -quark signal is large since there are 3 times as many pairs of W-bosons which could decay leptonically to give the signal. Unfortunately, in all cases the SM3 background, largely from top pairs, is so large that it obscures this signal by about an order of magnitude with the cuts we used in these plots.

In Figure 10 we plot the invariant mass spectrum for same sign dilepton pairs in the case of b' -quarks of mass 450 GeV and 600 GeV. As discussed in the previous section, the SM background here is not an issue.

The same sign dilepton signal should thus be a prominent signal for b' -quarks and from the cross-section and shape of the invariant mass spectrum, one should be able to infer the b' mass without considering the kinematics discussed below. In Table III we show the average invariant mass of the dilepton pairs, $\overline{m_{ll}}$ in the cases considered above. We

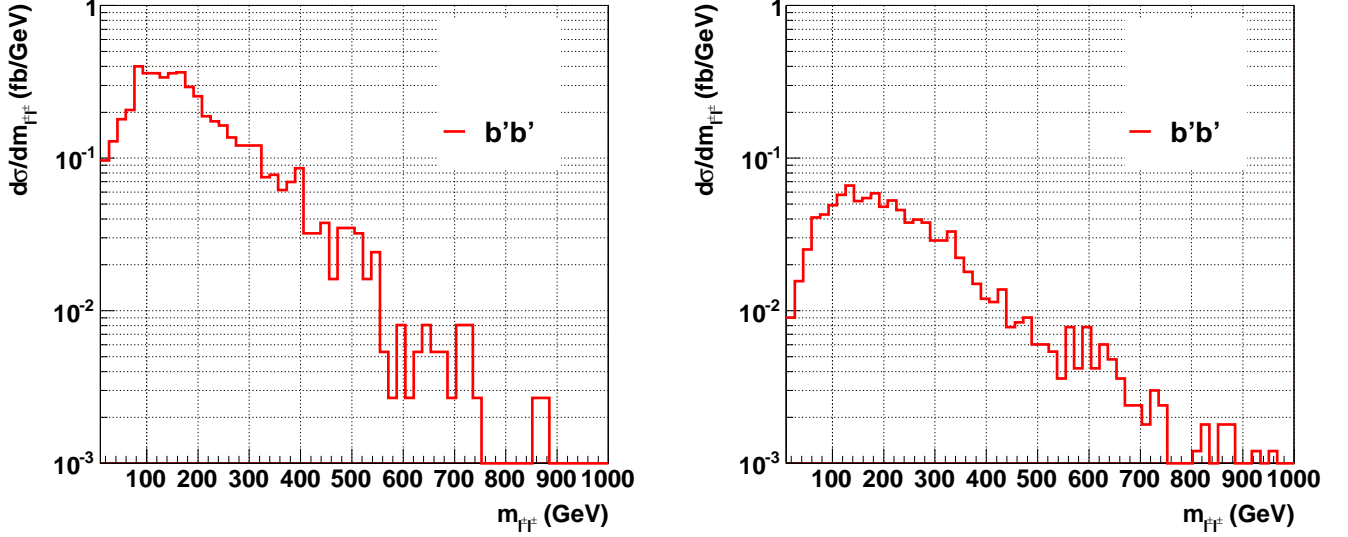


FIG. 10: $m_{l\pm l\pm}$ distributions for SSD (same sign dilepton) cases with $m_Q = 450$ (left), $m_Q = 600$ (right).

find that the ratio $\overline{m_{ll}}/m_Q$ is stable as a function of m_Q for each type of decay, in particular $\overline{m_{ll}}/m_Q \approx 0.54$ for OSD in t' -quark pairs; $\overline{m_{ll}}/m_Q \approx 0.40$ for OSD in b' -quark pairs and $\overline{m_{ll}}/m_Q \approx 0.42$ for SSD in b' -quark pairs.

Case	t' 450 GeV	t' 600 GeV	b' 450 GeV	b' 600 GeV	b' 400 GeV and t' 450 GeV	SM Background
OSD	255	313	182	236	220	197
SSD	N/A	N/A	195	245	N/A	N/A

TABLE III: The average dilepton mass for OSD (opposite sign dilepton) and SSD (same sign dilepton) cases. For the OSD case we consider t' -pair and b' -pair production as well as the Standard Model background. In the SSD case the background is negligible.

C. Analysis of Like Sign Dilepton Sample

Heavy quark production can contribute to this sample if it decays through channels 2-5 (See Eqns. 21 and 22). Under the assumptions we are using, this signal will arise from channel (2) which is the case when a b' undergoes two body tW decay and the cascade of the top quark gives the second W-boson.

In this case, we can in principle reconstruct both of the unobserved neutrino momenta provided we have the correct assignment of jets. To see how this works, consider the underlying topology of such an event:

$$\begin{aligned}
 b'_1 &\rightarrow W_1 t_1 \\
 &\hookrightarrow W_1 \rightarrow \ell_1 \nu_1 \\
 &\hookrightarrow t_1 \rightarrow jets \\
 b'_2 &\rightarrow W_2 t_2 \\
 &\hookrightarrow W_2 \rightarrow jets \\
 &\hookrightarrow t_2 \rightarrow b_2 W_3 \\
 &\hookrightarrow W_3 \rightarrow \ell_2 \nu_2
 \end{aligned} \tag{30}$$

Assuming that we have correctly assigned jets or sets of jets to the momenta t_1 , W_2 and b_2 , then the kinematic constraints are:

$$\begin{aligned}
m_W^2 &= (\ell_1 + \nu_1)^2 = (\ell_2 + \nu_2)^2 \\
m_t^2 &= (\ell_2 + \nu_2 + b_2)^2 \\
0 &= \nu_1^2 = \nu_2^2 \\
(\ell_1 + \nu_1 + t_1)^2 &= (\ell_2 + \nu_2 + b_2 + W_2)^2 \\
\not{p}_{x,y} &= (\nu_1 + \nu_2)_{x,y}
\end{aligned} \tag{31}$$

These kinematic constraints provide 8 equations for the 8 unknown components of ν_1 and ν_2 . In solving these equations there is in general a two fold or four fold ambiguity in addition to the combinatorial ambiguity.

If we take the events from this sample and analyze them in this way, then there will be a peak at the correct value of $m_{b'}$. Figure 11 shows a histogram of the b' mass reconstructed in this way for a number of different masses of the b' at $\sqrt{s} = 14$ TeV.

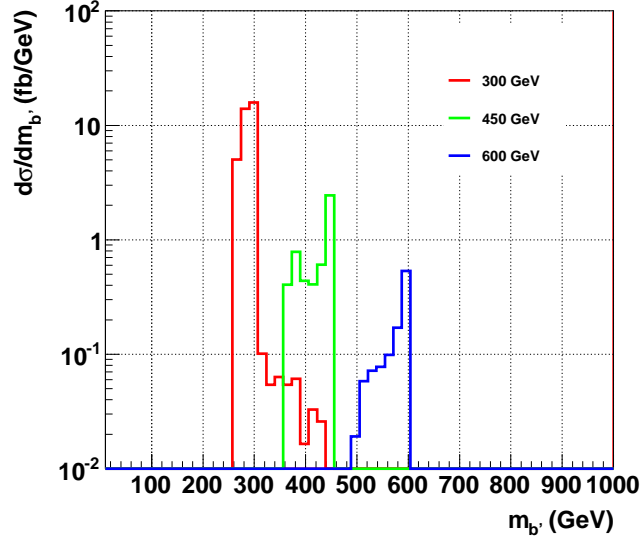


FIG. 11: The reconstructed b' masses from SSD (same sign dilepton) signal case at $\sqrt{s} = 14$ TeV [63].

D. Analysis of Opposite Sign Dilepton Sample

For the signal where opposite sign dileptons are produced, it is useful to distinguish three different scenarios, for how the leptons arise, which we will denote OSD1, OSD2 and OSD3. These scenarios vary in terms of the number of kinematic constraints which are available to reconstruct the mass of the heavy quark.

OSD1: The first scenario applies only in the case of b' production. In this case, it could happen that both of the leptons arise from top decay, for instance in the topology:

$$\begin{aligned}
b'_1 &\rightarrow W_1 t_1 \rightarrow \ell_1 \nu_1 b_1 \\
&\hookrightarrow W_1 \rightarrow jets \\
b'_2 &\rightarrow W_2 t_2 \rightarrow \ell_2 \nu_2 b_2 \\
&\hookrightarrow W_2 \rightarrow jets
\end{aligned} \tag{32}$$

Then the reconstruction of the event is overdetermined as in the case of the single lepton signal.

To see this, let us list the kinematic constraints:

$$\begin{aligned}
(b_1 + \ell_1 + \nu_1 + W_1)^2 &= (b_2 + \ell_2 + \nu_2 + W_2)^2 \quad (= m_Q^2) \\
m_W^2 &= (\ell_1 + \nu_1)^2 = (\ell_2 + \nu_2)^2 \\
m_t^2 &= (\ell_1 + \nu_1 + b_1)^2 = (\ell_2 + \nu_2 + b_2)^2 \\
(\nu_1 + \nu_2)_x &= \cancel{p}_x, \quad (\nu_1 + \nu_2)_y = \cancel{p}_y \\
0 &= \nu_1^2 = \nu_2^2
\end{aligned} \tag{33}$$

Here there are 9 equations to determine the 8 unknown components of ν_1 and ν_2 which is helpful in deciding if a given event is consistent with this topology. In Figure 12 we show a histogram of events reconstructed in this scenario at $\sqrt{s} = 14$ TeV.

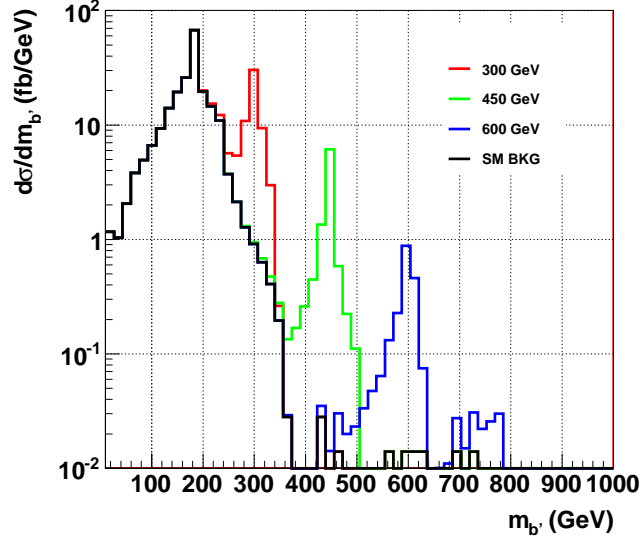


FIG. 12: Reconstructed b' mass from OSD (opposite sign dilepton) signal case 1 (OSD1) at $\sqrt{s} = 14$ TeV[63]. SM background is also presented.

OSD2: The second opposite sign dilepton scenario (OSD2) also applies to b' production where we assume that one of the b' quarks decays to jets and both of the leptons arise from the decay chain of the other. In the first case, if there is no merging between jets from the two heavy quarks, then for one of the partitions of the jets into j_h , the jets from the hadronic Q and j_ℓ , the jets from the leptonic Q , m_Q is given by $j_h^2 = m_Q^2$. As in the single lepton sample we can somewhat reduce the combinatorial background by noting that the correct partition of jets must satisfy the inequality:

$$j_h^2 > j_\ell^2 + 2m_W^2 + 2j_\ell \cdot (\ell_1 + \ell_2) \tag{34}$$

Thus if we construct a histogram of all jet partitions which satisfy this relation, there should be an accumulation at the correct value(s) of m_Q . In this analysis it is not necessary to decompose the missing momentum into the two individual neutrinos accompanying the two leptons. In Figure 13 we show a histogram of the reconstructed heavy quark mass in this scenario at $\sqrt{s} = 14$ TeV.

OSD3: The third opposite sign dilepton scenario (OSD3) is the most general. In this case we assume that the leptons are produced promptly from the initial heavy quark decays, for instance

$$\begin{aligned}
t' &\rightarrow b[W \rightarrow \ell\nu] \\
t' &\rightarrow b[W \rightarrow \ell\nu]
\end{aligned} \tag{35}$$

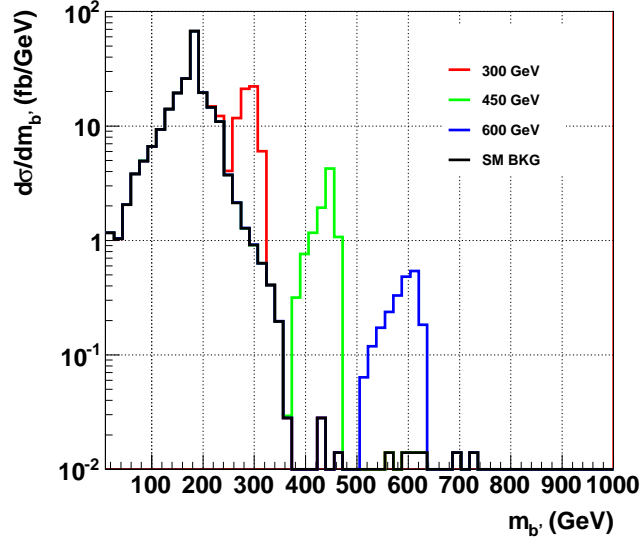


FIG. 13: Reconstructed b' masses from opposite sign dilepton signal case 2 (OSD2) at $\sqrt{s} = 14$ TeV[63]. SM background is also presented.

This scenario would therefore apply to both t' and b' pair production since overall we just assume that $Q \rightarrow [W \rightarrow \ell\nu] + jets$ on both sides of the event. Since there are no particles with known masses in the decay chain besides the W -bosons which produce the leptons, this is the least kinematically constrained case.

In general to reconstruct the heavy quark mass we need to reconstruct the neutrino momenta but in this case we do not have enough information to do so. This is evident because the kinematic constraints in this case are:

$$\begin{aligned}
 (j_1 + \ell_1 + \nu_1)^2 &= (j_2 + \ell_2 + \nu_2)^2 \quad (= m_Q^2) \\
 m_W^2 &= (\ell_1 + \nu_1)^2 = (\ell_2 + \nu_2)^2 \\
 0 &= \nu_1^2 = \nu_2^2 \\
 (\nu_1 + \nu_2)_x &= \cancel{p}_x \quad (\nu_1 + \nu_2)_y = \cancel{p}_y
 \end{aligned} \tag{36}$$

which provides only 7 constraints on the 8 unknown components of ν_1 and ν_2 and so we are one constraint short of what is required to fully reconstruct the event.

We can, however, take advantage of the kinematics of the heavy quark decay and obtain an approximate value of m_Q for an individual event. To do this, note that both the matrix element and structure functions of the proton tend to favor heavy quark production near threshold. If we make the approximation that the Q pair is at threshold, we can replace the first condition above with the following two conditions:

$$\begin{aligned}
 (j_1 + \ell_1 + \nu_1)_z &= (j_2 + \ell_2 + \nu_2)_z \\
 (j_1 + \ell_1 + \nu_1)_t &= (j_2 + \ell_2 + \nu_2)_t
 \end{aligned} \tag{37}$$

which then gives a total of eight conditions for the eight unknown components of ν_1 and ν_2 . If \tilde{m}_Q is the reconstructed mass of the Q based on this assumption, the accumulation of \tilde{m}_Q will give an indication of the true Q mass(es). Note that there is a two fold ambiguity in solving this system of equations. In Figure 14 we show a histogram of the reconstructed t' and b' masses in this scenario at $\sqrt{s} = 14$ TeV.

In the above three plots (Figures 12- 14), we have assumed that the topology which gives rise to the input was known. In reality, of course, we would not know which scenario might be producing a given event but rather we would have an event with jets plus an opposite sign dilepton passing the initial cuts. Our event sample would therefore be a mixture of OSD1, OSD2 and OSD3 events.

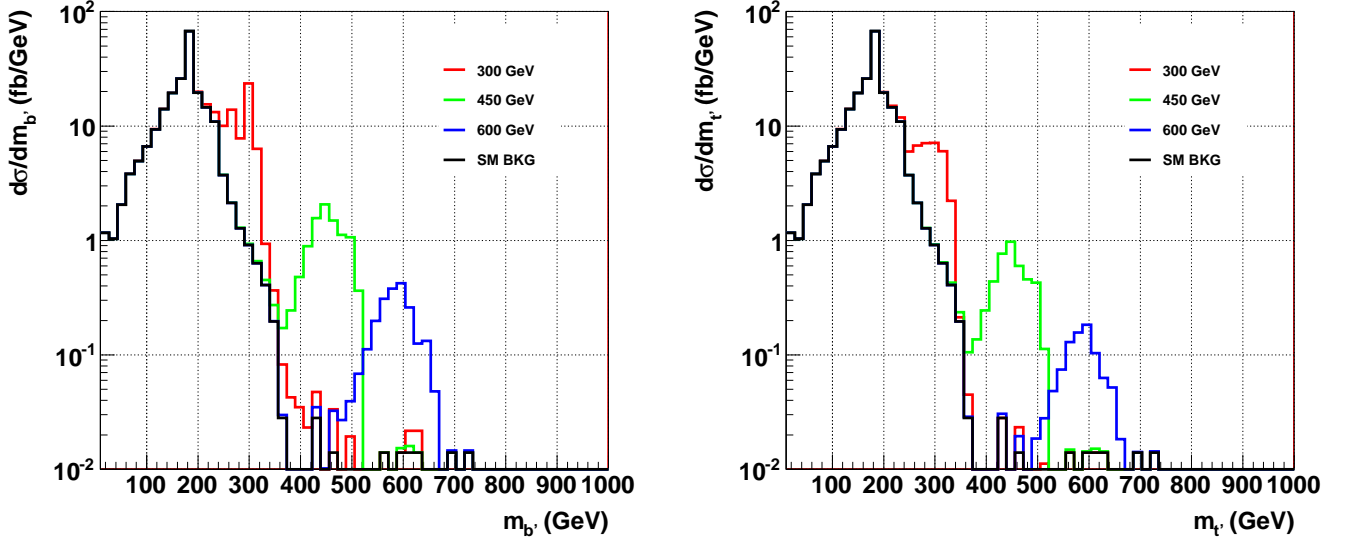


FIG. 14: Reconstructed t' and b' masses for opposite sign dilepton case 3 (OSD3) at $\sqrt{s} = 14$ TeV[63]. SM background is also presented.

To handle this situation let us consider the following approach: we take each event and analyze it as if it is, in turn, an OSD1 event, and OSD2 event and an OSD3 event. Thus for each event we potentially have three sets of reconstructed b' masses. In practice much of the time only the correct mode of analysis produces physical results. In any case, in Figure 15 we have used each of the three forms of analysis on each event in a sample of b' -quark pairs containing OSD1, OSD2 and OSD3 decay topologies and plotted a histogram of all the reconstructed masses which arise. A single event might contribute multiple points to the histogram. As can be seen, there is still reasonably strong peaking at the correct b' mass.

It is clear from the above Figures that the masses of t' and b' can be reconstructed within 10 percent accuracy in all the cases.

E. $2b + 6W$ signal

A very interesting signal arises when the $V_{t'b'}, V_{tb} \gg V_{t'b}$. In this case the branching ratio for $t' \rightarrow b'W^*$ will be $\simeq 1$. Now since b' decays into a top and a W boson, in case of t' - pair production, our signal will consist of $2b + 6W$'s. Below in Tables IV, V we present event rates for the cases when one or two W 's decay leptonically for two cases of the mass difference $\Delta m = m_{t'} - m_{b'} = 25$ GeV and 50 GeV respectively.

In Tables IV, V we note that event rate is lesser for smaller Δm . This is because the lepton/jets arising due to the decay of off-shell W 's will be relatively softer for smaller Δm and therefore these leptons/jets will suffer more from the p_T cuts on them.

IV. STANDARD MODEL BACKGROUNDS

The leading SM background for the aforementioned processes is due to top pair production, where at least one top decays semileptonically. To this end, in our analysis, we also include process where a top pair is produced with up to 3 jets, i.e. $tt + nj$; with $n \leq 3$. The other subdominant backgrounds that can affect our signal are due to tri-gauge boson production processes: VVV ; $V = W^\pm, Z$. It is to be noted that there can be other sources as well such as $ttVV$ and $VVVV$ but these will be quite small as compared to the aforementioned ones, therefore, we ignored such background in our analysis. We list all the relevant processes and their respective production cross-section in Table VI.

Clearly the jets or lepton arising due to the background processes will be relatively softer than our signal. Therefore, with the demand of higher transverse momentum jets and leptons or alternatively a higher scalar sum of transverse mo-

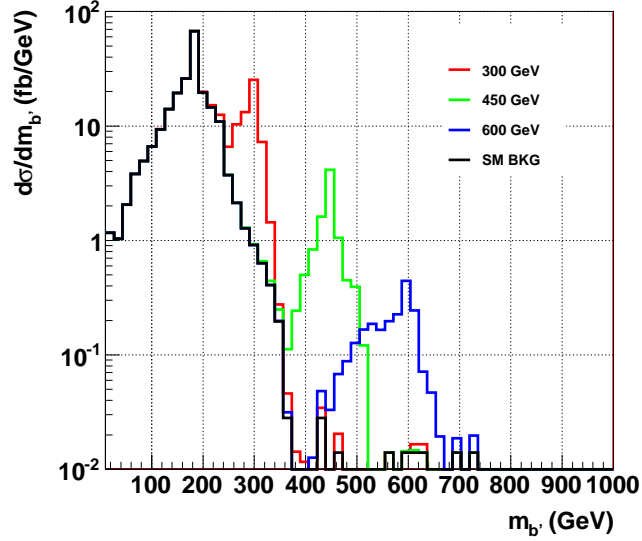


FIG. 15: Reconstructed b' masses where a mixture of OSD1, OSD2 and OSD3 events are analyzed using the three different methods, i.e. assuming that the event has OSD1, OSD2 and OSD3 topology at $\sqrt{s} = 14$ TeV[63]. SM background is also presented.

$\sqrt{s}(\text{TeV})$	cuts	$m_{t'} = 350$ GeV	$m_{t'} = 450$ GeV	$m_{t'} = 600$ GeV
		$m_{t'} - m_{b'} = 25$ GeV		
7	<i>Basic</i>	509, 84, 51	116, 19, 11	19, 3, 2
	<i>Basic</i> + $H_T > 350$ GeV	442, 72, 42	111, 18, 11	17, 3, 2
10	<i>Basic</i>	1655, 272, 159	413, 72, 43	77, 13, 9
	<i>Basic</i> + $H_T > 350$ GeV	1439, 235, 136	286, 69, 30	76, 13, 9
14	<i>Basic</i>	4516, 736, 477	1222, 222, 127	259, 45, 28
	<i>Basic</i> + $H_T > 350$ GeV	3942, 648, 423	1177, 213, 119	256, 44, 28
		$m_{t'} - m_{b'} = 50$ GeV		
7	<i>Basic</i>	534, 137, 87	119, 30, 21	18, 5, 3
	<i>Basic</i> + $H_T > 350$ GeV	445, 119, 75	114, 29, 20	18, 5, 3
10	<i>Basic</i>	1773, 432, 296	442, 118, 74	78, 21, 13
	<i>Basic</i> + $H_T > 350$ GeV	1501, 379, 254	421, 114, 71	77, 21, 13
14	<i>Basic</i>	4843, 1233, 754	1276, 344, 223	261, 72, 44
	<i>Basic</i> + $H_T > 350$ GeV	4093, 1079, 648	1223, 331, 214	258, 71, 44

TABLE IV: Number of signal and background single lepton, opposite sign dileptons (OSD), and same sign dileptons (SSD) events from the $t't'$ -pair production at the LHC from $t't' \rightarrow 2b + 6W$ state for $m_{t'} - m_{b'} = 25$ GeV and 50 GeV for $\sqrt{s} = 7, 10$ and 14 TeV and $\int \mathcal{L} dt = 1 \text{ fb}^{-1}$ without the requirement of isolation on jets. The basic cuts are the same as in Table I.

momentum of visible final state particles and the missing transverse energy, H_T will reduce the background considerably as shown in Tables I and II for each case.

V. SUMMARY AND CONCLUSIONS

Extending the Standard Model by adding a fourth fermion generation may be helpful in understanding how electro-weak symmetry breaking works and possibly also in elucidating the mechanism of baryogenesis in the early universe. The LHC will pair produce fourth generation quarks at a relatively high rate if their mass is in the range 400–600 GeV. Decay channels which result in final states with one or two leptons provide signals which have only modest Standard

$\sqrt{s}(\text{TeV})$	cuts	$m_{t'} = 350 \text{ GeV}$	$m_{t'} = 450 \text{ GeV}$	$m_{t'} = 600 \text{ GeV}$
		$m_{t'} - m_{b'} = 25 \text{ GeV}$		
7	<i>Basic</i>	417, 68, 41	97, 16, 9	15, 3, 2
	<i>Basic</i> + $H_T > 350 \text{ GeV}$	361, 58, 35	93, 15, 9	15, 3, 2
10	<i>Basic</i>	1334, 214, 125	354, 61, 36	65, 11, 7
	<i>Basic</i> + $H_T > 350 \text{ GeV}$	1156, 184, 108	340, 59, 35	64, 11, 7
14	<i>Basic</i>	3801, 629, 399	1042, 188, 109	225, 39, 24
	<i>Basic</i> + $H_T > 350 \text{ GeV}$	3317, 552, 354	1004, 181, 103	222, 38, 23
		$m_{t'} - m_{b'} = 50 \text{ GeV}$		
7	<i>Basic</i>	443, 113, 73	99, 25, 17	15, 4, 3
	<i>Basic</i> + $H_T > 350 \text{ GeV}$	368, 97, 61	95, 24, 17	15, 4, 3
10	<i>Basic</i>	1467, 353, 244	367, 98, 60	66, 18, 11
	<i>Basic</i> + $H_T > 350 \text{ GeV}$	1236, 309, 210	351, 94, 58	65, 18, 11
14	<i>Basic</i>	3954, 997, 626	1067, 289, 186	222, 61, 39
	<i>Basic</i> + $H_T > 350 \text{ GeV}$	3327, 871, 540	1024, 279, 178	222, 60, 38

TABLE V: This table shows the number of events with the same cuts as in Table IV with the addition of the jet isolation cut that all the jets are separated with $\Delta R_{jj} > 0.4$.

SM Background	$t\bar{t} + 0j$	$t\bar{t} + 1j$	$t\bar{t} + 2j$	$t\bar{t} + 3j$	$t\bar{t}V$	VVV
7 TeV	89.7	20.7	19.4	10.2	0.24	0.06
10 TeV	233.6	64.2	60.2	23.3	0.57	0.12
14 TeV	535.1	443.2	247.3	108.3	1.2	0.21

TABLE VI: Cross-section (in pb) for various SM background processes at the LHC with $\sqrt{s} = 7, 10$ and 14 TeV with basis cuts.

Model backgrounds.

In this study we considered the case where fourth generation quarks decay predominantly to quarks from the first three generations assuming that the mass splitting between the fourth generation quarks is small. This is likely the decay mechanism of the lightest fourth generation quark and also could be the decay mode for both of the heavy quarks. For such a quark we investigated the signals and backgrounds in three different channels: (1) Single lepton plus jets and missing momentum; (2) Opposite sign dilepton pair plus jets and missing momentum and (3) Same sign dilepton pair plus jets and missing momentum. In all cases, we first consider a basic set of cuts which eliminates a large portion of the background but generally leaves the signal intact. To further isolate the signal we use the kinematics of the event to reconstruct the heavy quark mass.

In the case of a single lepton plus jets and missing momentum, we can use the fact that the missing momentum arises from a single neutrino which is associated with the lepton in the decay of a W -boson. This constraint over determines the kinematics once the role of the jets is correctly assigned. In particular one can extract independently a mass for the heavy quark both from the hadronic and leptonic sides of the event. We find that the combinatorial background from the many possible jet assignments can be greatly reduced if you accept only the jet assignment which minimizes the discrepancy between the two mass determinations. Other cuts which are helpful in reducing the combinatorial background are a cut on H_T and a cut on Δm_W which tends to force jet pairs which arise from the decay of a single W boson to be assigned to the same side of the event.

If the single lepton event arises from the decay of a heavy quark to a light quark other than the top (i.e. which we have generally taken to be a t' in our discussion), there are a total of four jets in the final state so the combinatorial background is not particularly severe. If, however a b' quark decays to a tW final state, then there are eight jets in total and the combinatorial background may pose a problem for quarks in the heavier mass range. Thus we have considered what mass resolution is required in order to satisfactorily implement the minimum Δm_Q selection of the correct jet assignment.

In the case of an opposite sign dilepton pair, if the heavy quark does not decay to a top quark, there are only 2 jets so there is no large combinatorial background; however, the kinematics of such events is underdetermined so the quark mass cannot precisely be extracted on an event by event basis. But if we make the approximation that the two heavy quarks are at rest in their center of mass frame, we can deduce roughly the heavy quark mass which evidently separates the signal from the background well enough to provide a prominent signal and determine the heavy quark mass.

In the case where a b' decays to tW there are three cases which could apply depending on whether 0, 1 or 2 of

the leptons arise from top decay. For each lepton which arises from top decay there is an additional constraint on the momentum of the associated neutrino; therefore, in these scenarios the kinematics is either under determined, critically determined or over determined respectively. For a given event we do not initially know which of these scenarios applies, however, if we iterate over the three scenarios and all jet assignments, most of the wrong assignments lead to unphysical neutrino momenta so that retaining the cases which can be reconstructed we produce a satisfactory signal and reconstruction of the heavy quark mass.

The same sign dilepton signal only arises in the scenario where $b' \rightarrow tW$ and results in kinematics where the neutrino momenta are critically determined. This channel has the advantage that the Standard Model background is negligible. As in the opposite sign case, we can resolve the combinatorial background by taking only cases where there are physical solutions for the neutrino momenta and thus obtain the heavy quark mass. Thus the mass of the heavy quark may be determined by the kinematic reconstruction or through the characteristics of the invariant mass distribution of the dilepton pair.

Acknowledgements

We would like to thank Michael Begel, Shaouly Bar-Shalom, Thomas Gadfort, Michael Wilson and Daniel Whiteson for discussions. In addition S. K. G. would like to thank Nils Krumnack and Marzia Rosati for their useful help with the package ROOT [62]. The work of D. A., S. K. G. and A. S. are supported in part by US DOE grant Nos. DE-FG02-94ER40817 (ISU) and DE-AC02-98CH10886 (BNL).

-
- [1] N. Cabibbo, Phys. Rev. Lett. **10**, 531 (1963).
 - [2] M. Kobayashi and T. Maskawa, Prog. Theor. Phys. **49**, 652 (1973).
 - [3] E. Lunghi and A. Soni, JHEP **0709**, 053 (2007) [arXiv:0707.0212 [hep-ph]].
 - [4] E. Lunghi and A. Soni, Phys. Lett. B **666**, 162 (2008) [arXiv:0803.4340 [hep-ph]]; E. Lunghi and A. Soni, Phys. Lett. B **697**, 323 (2011) [arXiv:1010.6069 [hep-ph]].
 - [5] E. Lunghi and A. Soni, JHEP **0908**, 051 (2009) [arXiv:0903.5059 [hep-ph]].
 - [6] A. Lenz and U. Nierste, JHEP **0706**, 072 (2007) [arXiv:hep-ph/0612167].
 - [7] M. Bona *et al.* [UTfit Collaboration], arXiv:0803.0659 [hep-ph].
 - [8] M. Bona *et al.* [UTfit Collaboration], Phys. Lett. **B687**, 61-69 (2010). [arXiv:0908.3470 [hep-ph]]; A. Lenz, *et. al.* Phys. Rev. **D83**, 036004 (2011). [arXiv:1008.1593 [hep-ph]].
 - [9] K. Agashe, G. Perez and A. Soni, Phys. Rev. Lett. **93**, 201804 (2004) [arXiv:hep-ph/0406101].
 - [10] K. Agashe, G. Perez and A. Soni, Phys. Rev. D **71**, 016002 (2005) [arXiv:hep-ph/0408134].
 - [11] M. Blanke, A. J. Buras, B. Duling, S. Gori and A. Weiler, JHEP **0903**, 001 (2009) [arXiv:0809.1073 [hep-ph]].
 - [12] M. Blanke, A. J. Buras, B. Duling, K. Gemmler and S. Gori, JHEP **0903**, 108 (2009) [arXiv:0812.3803 [hep-ph]].
 - [13] M. Bauer, S. Casagrande, U. Haisch, M. Neubert, JHEP **1009**, 017 (2010). [arXiv:0912.1625 [hep-ph]].
 - [14] V. Barger, L. L. Everett, J. Jiang, P. Langacker, T. Liu and C. E. M. Wagner, JHEP **0912**, 048 (2009) [arXiv:0906.3745 [hep-ph]].
 - [15] W. Altmannshofer, A. J. Buras, S. Gori, P. Paradisi and D. M. Straub, Nucl. Phys. B **830**, 17 (2010) [arXiv:0909.1333 [hep-ph]].
 - [16] P. Q. Hung, M. Sher, Phys. Rev. **D77**, 037302 (2008). [arXiv:0711.4353 [hep-ph]].
 - [17] P. H. Frampton, P. Q. Hung, M. Sher, Phys. Rept. **330**, 263 (2000). [hep-ph/9903387].
 - [18] A. Soni, A. K. Alok, A. Giri, R. Mohanta and S. Nandi, arXiv:1002.0595 [hep-ph].
 - [19] A. Soni, A. K. Alok, A. Giri, R. Mohanta and S. Nandi, Phys. Lett. B **683**, 302(2010) [arXiv:0807.1971]; S. Nandi and A. Soni, arXiv:1011.6091 [hep-ph].
 - [20] A. Buras *et al.*, JHEP **1009**, 106 (2010) [arXiv:1002.2126].
 - [21] W. S. Hou and C. Y. Ma, Phys. Rev. D **82**, 036002, 2010 [arXiv:1004.2186].
 - [22] O. Eberhardt, A. Lenz, J. Rohrwild, Phys. Rev. **D82**, 095006 (2010). [arXiv:1005.3505 [hep-ph]].
 - [23] K. Agashe, A. Delgado, M. May and R. Sundrum, JHEP **0308**, 050, 2003; [hep-ph/0308036].
 - [24] K. Agashe, H. Davoudiasl, G. Perez and A. Soni, Phys. Rev. **D75**, 015002, 2007.
 - [25] K. Agashe *et al.*, Phys. Rev. **D76**, 115015, [arXiv:0709.0007].
 - [26] K. Agashe *et al.*, Phys. Rev. **D80**, 075007, 2009; [arXiv:0810.1497].
 - [27] M. Cacciari *et al.*, JHEP **0809**, 127, 2008 [arXiv: 0804.2800].
 - [28] See the talk by Daniel Whiteson at the NTU workshop, Jan 2010.
 - [29] M. S. Chanowitz, M. A. Furman, I. Hinchliffe, Nucl. Phys. **B153**, 402 (1979); *ibid.* Phys. Lett. **B78**, 285 (1978).
 - [30] Z. Murdock, S. Nandi and Z. Tavartkiladze, Phys. Lett. B **668**, 303 (2008) [arXiv:0806.2064 [hep-ph]].
 - [31] See the talk by P. Murat on "Searches Beyond the Standard Model" at the Fermilab Tevatron at the ICEHEP 2010 (Paris).
 - [32] See the talk by John Conway at the Brookhaven Forum 2010.

- [33] T. Aaltonen *et al.*, CDF Collab, Phys. Rev. Lett. 104, 0911801, 2010; arXiv:0912.1057;
- [34] T. Aaltonen *et al.* [The CDF Collaboration], Phys. Rev. Lett. **106**, 141803 (2011). [arXiv:1101.5728 [hep-ex]].
- [35] V. M. Abazov *et al.* [D0 Collaboration], [arXiv:1104.4522 [hep-ex]].
- [36] S. Chatrchyan *et al.* [CMS Collaboration], [arXiv:1102.4746 [hep-ex]].
- [37] K. Nakamura *et al.* [Particle Data Group], J. Phys. G **37**, 075021 (2010).
- [38] H. -J. He, N. Polonsky, S. -f. Su, Phys. Rev. **D64**, 053004 (2001); V. A. Novikov, L. B. Okun, A. N. Rozanov, M. I. Vysotsky, Phys. Lett. **B529**, 111-116 (2002); [hep-ph/0111028]; V. A. Novikov, L. B. Okun, A. N. Rozanov, M. I. Vysotsky, JETP Lett. **76**, 127-130 (2002). [hep-ph/0203132]; G. D. Kribs, T. Plehn, M. Spannowsky, T. M. P. Tait, Phys. Rev. **D76**, 075016 (2007). [arXiv:0706.3718 [hep-ph]]; J. Erler, P. Langacker, Acta Phys. Polon. **B39**, 2595-2610 (2008). [arXiv:0807.3023 [hep-ph]]; M. S. Chanowitz, Phys. Rev. **D79**, 113008 (2009). [arXiv:0904.3570 [hep-ph]]; M. S. Chanowitz, Phys. Rev. **D**, 035018 (2010) [arXiv:1007.0043 [hep-ph]].
- [39] B. Holdom, W. S. Hou, T. Hurth, M. L. Mangano, S. Sultansoy and G. Unel, PMC Phys. A **3**, 4 (2009) [arXiv:0904.4698 [hep-ph]]; M. Hashimoto, V. A. Miransky, Phys. Rev. **D81**, 055014 (2010). [arXiv:0912.4453 [hep-ph]]. B. Holdom, Phys. Lett. **B686**, 146-151 (2010). [arXiv:1001.5321 [hep-ph]].
- [40] B. Holdom, Phys. Rev. Lett. **57**, 2496 (1986) [Erratum-ibid. **58**, 177 (1987)].
- [41] S. F. King, Phys. Lett. B **234**, 108 (1990).
- [42] C. T. Hill, M. A. Luty and E. A. Paschos, Phys. Rev. D **43**, 3011 (1991).
- [43] J. Carpenter, R. Norton, S. Siegemund-Broka and A. Soni, Phys. Rev. Lett. **65**, 153 (1990).
- [44] P. Q. Hung and C. Xiong, arXiv:0911.3890 [hep-ph].
- [45] P. Q. Hung, C. Xiong, Nucl. Phys. **B848**, 288-302 (2011). [arXiv:1012.4479 [hep-ph]].
- [46] G. Burdman, L. Da Rold, JHEP **0712**, 086 (2007). [arXiv:0710.0623 [hep-ph]].
- [47] W. S. Hou, Chin. J. Phys. **47**, 134 (2009) [arXiv:0803.1234 [hep-ph]].
- [48] S. W. Ham, S. K. Oh and D. Son, Phys. Rev. D **71**, 015001 (2005) [arXiv:hep-ph/0411012].
- [49] R. Fok and G. D. Kribs, Phys. Rev. D **78**, 075023 (2008) [arXiv:0803.4207 [hep-ph]].
- [50] Y. Kikukawa, M. Kohda and J. Yasuda, Prog. Theor. Phys. **122**, 401 (2009) [arXiv:0901.1962 [hep-ph]].
- [51] A. D. Sakharov, Pisma Zh. Eksp. Teor. Fiz. **5**, 32-35 (1967).
- [52] T. Gershon, A. Soni, J. Phys. G **G33**, 479-492 (2007). [hep-ph/0607230].
- [53] G. Eilam, B. Melic and J. Trampetic, Phys. Rev. D **80**, 116003 (2009) [arXiv:0909.3227 [hep-ph]].
- [54] D. Das, D. London, R. Sinha, A. Soffer, Phys. Rev. **D82**, 093019 (2010). [arXiv:1008.4925 [hep-ph]].
- [55] A. Arhrib, W. -S. Hou, JHEP **0607**, 009 (2006). [hep-ph/0602035].
- [56] See also B. Holdom, JHEP **0708**, 069 (2007). [arXiv:0705.1736 [hep-ph]]; B. Holdom, Q. -S. Yan, [arXiv:1004.3031 [hep-ph]].
- [57] Y. Chao, K. -F. Chen, S. -K. Chen, W. -S. Hou, B. -Y. Huang, Y. -J. Lei, [arXiv:1101.0592 [hep-ph]].
- [58] T. Stelzer and W. F. Long, Comput. Phys. Commun. **81**, 357 (1994) [arXiv:hep-ph/9401258]; J. Alwall *et al.*, JHEP **0709**, 028 (2007) [arXiv:0706.2334 [hep-ph]]; J. Alwall, P. Artoisenet, S. de Visscher, C. Duhr, R. Frederix, M. Herquet and O. Mattelaer, AIP Conf. Proc. **1078**, 84 (2009) [arXiv:0809.2410 [hep-ph]].
- [59] T. Sjostrand, S. Mrenna and P. Z. Skands, JHEP **0605**, 026 (2006) [arXiv:hep-ph/0603175].
- [60] J. Pumplin, D. R. Stump, J. Huston, H. L. Lai, P. M. Nadolsky and W. K. Tung, JHEP **0207**, 012 (2002) [arXiv:hep-ph/0201195].
- [61] B. Holdom, Q. -S. Yan, [arXiv:1101.3844 [hep-ph]].
- [62] R. Brun, F. Rademakers, Nucl. Instrum. Meth. **A389**, 81-86 (1997).
- [63] For clarity, we show the invariant mass distributions for $\sqrt{s} = 14$ TeV only. The invariant mass distributions for $\sqrt{s} = 7 - 14$ TeV generally have the same shape but are rescaled by the total cross section.